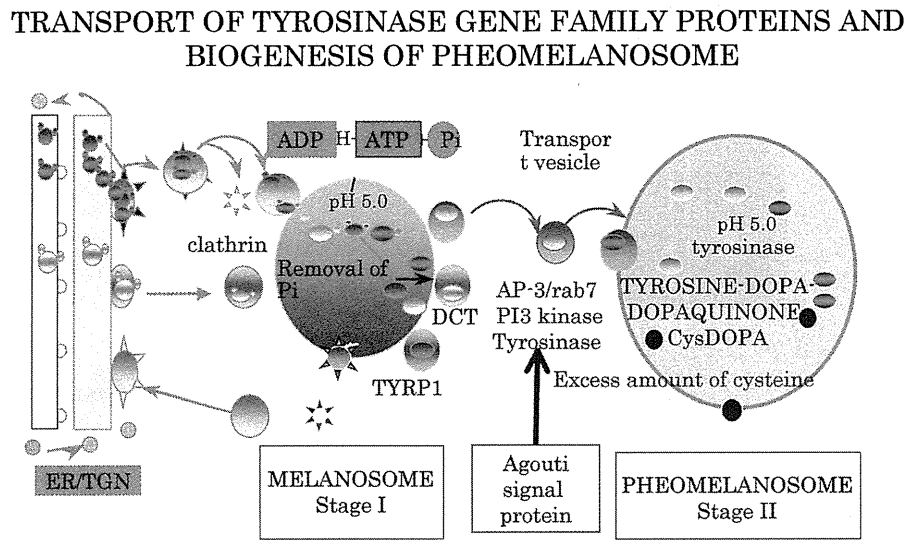

Figure 7: Vesicular transport of tyrosinase and biogenesis of pheomelanosomes.

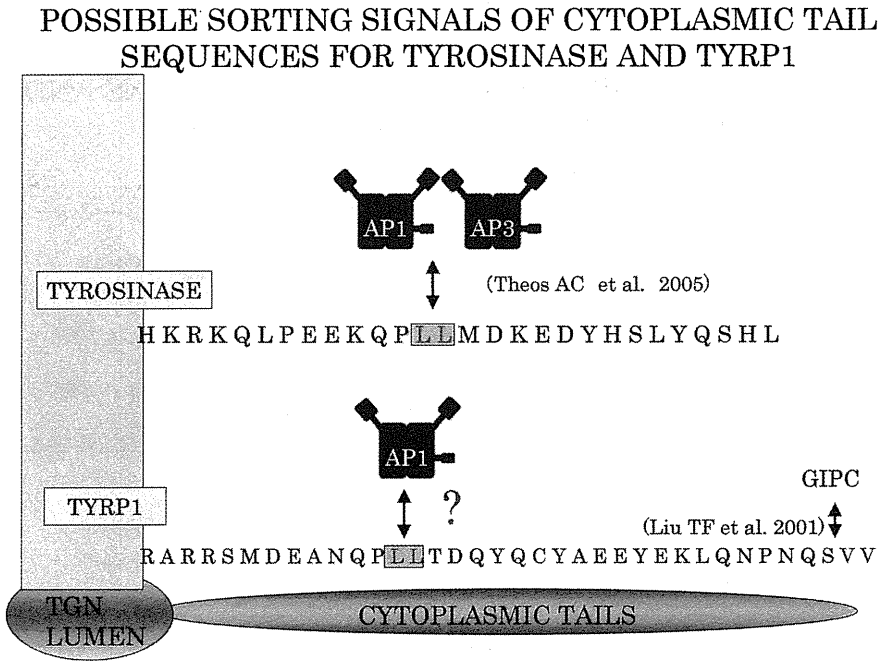

Figure 8: Possible sorting signals of cytoplasmic tail sequences for tyrosinase and TYRP 1. Cytoplasmic tail motifs of tyrosinase and TYRP 1 are referred from the reports of Theos AC et al. and Liu TF et al. respectively.[21,36]

Both tyrosinase and TYRP 1 are transported from the trans-Golgi network (TGN) to melanosomes via endosomal compartments (Fig. 6, 7). Adaptor proteins (APs) generate transport vesicles, sorting proteins and assembling clathrin to the local membrane in endosomes.[42] AP 3, one of the four known mammalian APs, has been reported to bind to a dileucine motif of tyrosinase.[5,14] A mutation of β 3 A subunit in AP 3 results in Hermansky-Pudlak syndrome (HPS)-2 in humans and pearl in mice.[8] Accumulating evidence suggests that both tyrosinase and TYRP 1 interact with APs and travel from endosomes to melanosomes, though the exact transport pathway is still not clear. It has recently been reported that tyrosinase can use both AP 1 and AP 3 for its proper sorting while TYRP 1 can use only AP 1.[53] It is also clear that

both tyrosinase and TYRP 1 are not transported to lysosomes. Tyrosinase may, however, be dedraded in lysosomes if its transport from TGN to melanosomes is blocked.[10]

3. Eumelanin biosynthesis and biological role of tyrosinase-related proteins

Mutations that effect different stages of melanocyte development have been best characterized in experimental mice. Both albino mutation of mouse tyrosinase and brown mutation of tyrosinase-related protein 1 (Tyrp-1) alter cysteine in the EGF motif to serine in albino mutation and different cysteine to tyrosine in brown mutation. Proof of the mutation status of the alteration has, in both cases, been provided by analysis of revertants which restore wild type function. In addition, comparison of the phenotypes with those of deletion of the loci indicates that both mutations have complete loss of function of the gene product. On the other hand, Tyrp-2 containing the slaty mutation, which has arginine to glutamine change at the first copper -binding sites may still have considerable DCT activity (Fig 8).

The function of TYRP/ tyrp-1 is still not fully understood, however, it is believed to be involved in eumelanin synthesis since the brown mutation only affects the eumelanic animals. It has shown that demonstrated gene changes in Tyrp-1 mRNA expression and in Tyrp-1 gene structure in certain mouse brown b-locus mutants. These findings have provided additional evidence of allelism and allowed an explanation of the phenotypes. The human homologue of TYRP-1 of the mouse brown gene maps to the short arm of chromosome 9 and extends the known region of homology with mouse chromosome 4.

Both recessive and dominant mutations of Tyrp-1 gene have been examined. Some recessive mutations involve single amino acid substitutions, changing an arginine residue to the single sequence cysteine, whereas others affect the levels of Tyrp-1 mRNA present in the melanocytes. These different mutations result in either complete loss of function, partial loss of function or temperature sensitive function. Dominant mutations affecting the Tyrp-1 gene have also arisen as a result of a base pair mutation. This type of mutation may destabilize the melanosomal membrane and allow the intermediates of

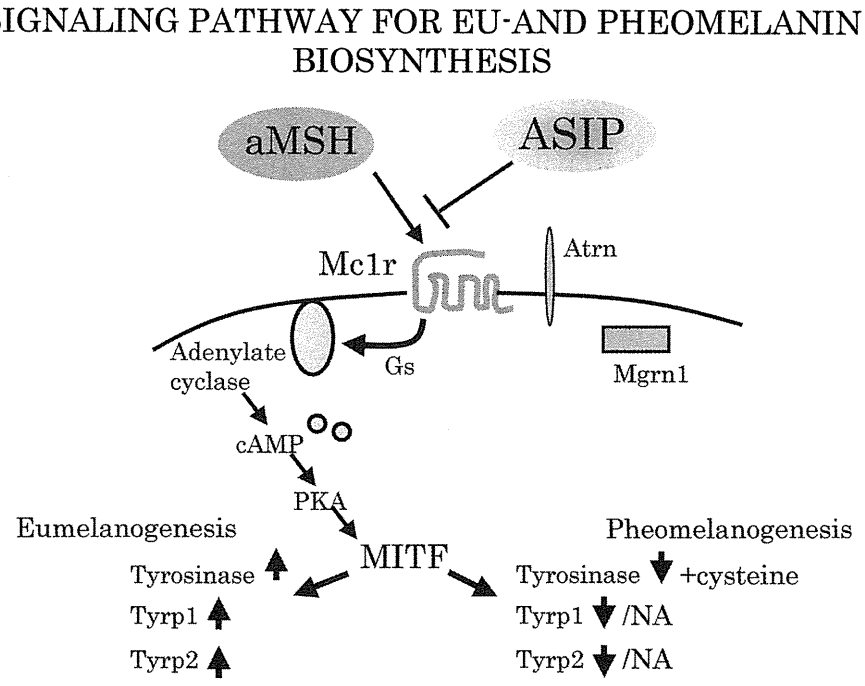

Figure 9: Agouti signaling protein is the key protein molecule which is involved in pheomelanin biosynthesis and which antagonizes to largely unknown MSH binding with Mc 1 r (melanocortin 1 receptor) on the melanocyte cell membrane. Attractin (Atrn) binds N terminal of Agouti/ASIP and supports this binding to Mc 1 r. Biological role of mahogunin (Mgrn) is still unknown.

melanogenesis, which are normally sequestered in the melanosomal compartment, to interfere with normal melanocyte function. Another type of dominant mutation may arise due to the Tyrp-1 gene having undergone some rearrangement, as a result Tyrp-1 is not properly transcribed, leading to melanocyte dysfunction and death. It has been therefore suggested that mutant TYRP-1 protein is involved in toxicity of melanocytes which is associated with inherently toxic melanogenesis process.[20,23]

4. Pheomelanin biosynthesis and its elevation in melanoma and dysplastic nevi

The diverse patterns of mammalian coat color are determined by the quantity and distribution of just two types of organic pigment: eumelanin (black to brown) and pheomelanin (yellow to red). Both are produced by melanocytes in the skin and hair.[20,21] Two major loci are central to pigment-type switching in mouse. One is the agouti locus encoding agouti signal protein (ASIP), with mutants including non-agouti(*a*), giving a eumelanic black mouse in the absence of other mutations) and dominant yellow (*Ay*) ; the other is the melanocortin-1 receptor (*Mc 1 r*) locus, formerly extension (*e*), also with both eumelanic and pheomelanic mutants (e.g. recessive yellow, $Mc1r^{e}$) (Fig. 9). MC 1 R is a cell-surface G-protein-coupled receptor for which the best-known agonist is the soluble peptide αMSH, cleaved from the precursor pro-opiomelanocortin (POMC) in the pituitary and skin. Binding of αMSH to MC 1 R is known to activate adenylate cyclase and cAMP synthesis, promoting eumelanin synthesis through both post-translational and transcriptional pathways via microphthalmia-related transcription factor (MITF).[3] MITF is a master regulator for eumelanogenesis, melanocyte differentiation, proliferation and survival. It promotes transcription of melanocyte-specific gene products including melanosomal enzymes tyrosinase, TYRP 1 and DCT and the matrix protein SILV/PMEL. Synthesis of both eumelanin and pheomelanin start from tyrosine oxidation catalyzed by tyrosinase. The resulting dopaquinone can be a substrate for eumelanin synthesis, promoted by TYRP 1 and DCT, or pheomelanin in the presence of high cysteine concentrations and/or low tyrosinase activity.

ASIP is a soluble protein of 131 amino acids, apparently secreted by dermal papilla cells in hair bulbs. It competitively antagonizes αMSH at the MC 1 R and inhibits the eumelanogenic signal, down regulating melanogenic enzymes

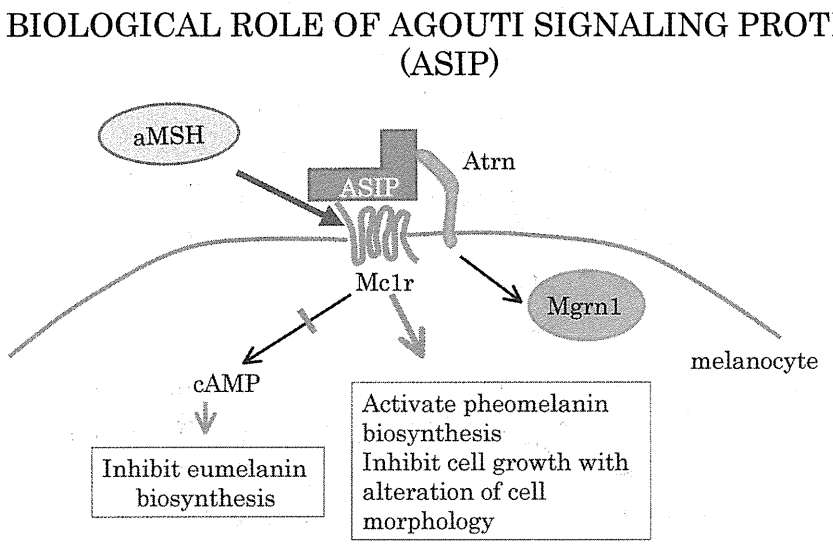

Figure 10: Activation of ASIP will result in not only eumelanin production inhibition and pheomelanin production activation but also the differentiation and proliferation of melanocyte. It is likely that there is an alternating signal transduction cascade beside cAMP cascade in this process.
This un-clarified, new cascade passes through Mc 1 r but is independent to cAMP cascade and does not include the pathway of Attractin (Atrn)/ mahogunin 1 (Mgrn 1).

and leading to pheomelanin synthesis (Fig. 10). For better understanding of ASIP signaling, we have sought to develop culture conditions under which ASIP contributes to overt pheomelanin synthesis by the melan-a immortal murine melanocyte line.[11]It was demonstrated that ASIP signaling can be reduced melanocyte growth and induce morphological dedifferentiation as well as affecting pigmentation (Fig. 10). These biological effects are mimicked in genetically yellow melanocytes, incomplete in Atrn- and *Mgrn1*-null melanocytes, appear independent of cAMP down-regulation, and require the amino terminus of ASIP.

As discussed in our previous report [18], significantly high content of pheomelanin was found in melanoma and dysplastic melanocytic nevi (DMN) lesions by analysis using high-pressure liquid chromatography (HPLC) [2,4,15-17,26,45], indicating that these abnormal melanosomes may be pheomelanic.[44,52] Our previous electron microscopic studies showed that melanocytes of dysplastic melanocytic nevi DMN were rich in abnormal melanosomes which exhibited features consistent with pheomelanosomes. It would be important to examine the type of melanogenesis in abnormal pigmentation in the aged skin such as senile freckle and solar lentigo. [11]

3. UV-photoproducts of pheomelanin and its precursors, and enhancement of skin aging process

Catalase structure and activity was seriously affected by photo-oxidation of its own substrates, hydrogen peroxide, owing to cleavage of its porphyrin active site.[2,54] Recently the over-expression of mitochondrial catalase in the murine model increased the lifespan of the mice by 40%, indicating the importance of this enzyme in the aging process.[47,54] UVA-irradiated pheomelanin altered the structure of catalase and decreased its activity in human skin.[35] Electron-spin resonance spectroscopy experiments by Sealy et al. on black and red melanin, suggested that red melanin (pheomelanin) contained a specific kind of free radical (s) not present in black eumelanin.[46]Chedekel et al. found that pheomelanin was photo-destroyed, in the presence of oxygen, by UVR.[5] Haryanvi et al., using the reversion test of Ames, demonstrated that pheomelanin became mutagenic after exposure to UVR.[11] Koch, Chedekel and Meresca et al. described photo-initiated DNA damage by melanogenic intermediates of 5-S-cysteinyldopa origin.[30,35] The binding of these molecules to DNA was activated by 300 nm UVR and resulted in single-strand breaks. However, while biosynthesis process and biological role of eumelanin after exposure to UVR are well characterized, the nature and photo-biological role of pheomelanin may still be largely unknown.

Summary and Perspective

Melanin pigmentation of the skin has been generally regarded to possess a protective role against exposure to UVR. Melanin pigment, specifically eumelanin, may therefore provide a protective role against development of sunburn, solar degeneration and skin aging as well as cancer.[24,25] Evidence accumulated recently indicates that the photoprotective role of the melanin pigment may be restricted to eumelanin as well as to the visible and UVA ranges and that in the UVB and UVC ranges both eumelanin and pheomelanin components may behave as photosensitizers. UV photolysis studies using catechols, catecholmines, and hydroxylated indole derivative (i.e., the eumelanin precursors) have demonstrated the formation of hydrated electrons, hydrogen atoms, semiquinone/ semiquinone imine radicals, and indoloxyl radicals. The photolysis of pheomelanin precursors leads to the formation of hydrated electrons, hydrogen atoms, and to alanyl and aryl thiyl radicals. Thus, while eumelanin may act as a photoprotector, its precursors may be still phototoxic.

The photoprotection by melanin pigment can be accomplished by scavenging the reactive free radicals, by quenching excited states, and by decreasing oxygen concentration in exposed tissues. The phototoxicity is related to the generation of reactive free radicals by low molecular eumelanic and pheomelanic intermediates. It may, however, be possible to modulate the photosensitivity of the pigmentary system by affecting the redox status of endogenous melanin pigments, or by switching melanin pigmentation from eumelanogensis to pheomelanogenesis, or *vice versa*, or by using sensitizers activated by red light, which is poorly absorbed by melanin.

Further investigation of the biological role in eu- and pheomelanin biosynthesis after UVR is required to provide a new insight for the better understanding the skin aging process.

Acknowledgment

This study was supported by the Ministry of Health, Labour and Welfare, Japan (H 21-Nano-006).

References

1) Al-Kazwini AT, O'Neill P, Adams GE, Cundall RB, Jacquet B, Lang G, Junino A: One-electron oxidation of methoxylated and hydroxylated indoles by N 3. 1. Characterization of the primary indolic radicals. JPhys Chem. 94: 6666-6670, 1990.
2) Aubert C, Rouge F, Galindo JR: Tumorigenicity of human malignant melanocytes in nude mice in relation to their differentiation in vitro. J Natl Cancer Inst. 64: 1029, 1980.
3) Bennett DC: Human melanocyte senescence and melanoma susceptibility genes. Oncogene. 19: 3063-3069, 2003.
4) Burchill SA, Thody AJ, Ito S: Melanocyte-stimulating hormone, tyrosinase activity and the regulation of eumelanogenesis and phaeomelanogenesis in the hair follicular melanocytes of the mouse. J Endocr. 109: 15-21.1986.
5) Calvo PA, Frank DW, Bieler BM, Berson JF, Marks MS: A cytoplasmic sequence in human tyrosinase defines a second class of di-leucine-based sorting signals for late endosomal and lysosomal delivery. J Bio Chem. 274: 12780-1279, 1999.
6) Chedekel MR, Post PW, Deibel RM, Kalus M: Photodestruction of phaeomelanin. Photochem Photobiol. 26: 651, 1977.
7) DeFelippis MR, Murthy CP, Faraggi M, Klapper MH: Pulse radiolysis measurement of redox potentials: the tyrosine and tryptophan radicals. Biochem. 28: 4847-4853, 1989.
8) Dell'Angelica EC, Shotelersuk V, Aguilar RC, Gahl WA, Bonifacino JS: Altered trafficking of lysosomal proteins in Hermansky-Pudlak syndrome due to mutations in the beta 3 A subunit of the AP-3 adaptor. Mol Cell. 3: 11-21, 1999.
9) d'Ischia M, Prota G: Photooxidation of 5,6-dihydroxy-1-methyl-indole. Tetrahedron. 43: 431-434, 1987.
10) Fujita H, Motokawa T, Katagiri T, Yokota S, Yamamoto A, Himeno M, Tanaka Y: Inulavosin, a melanogenesis inhibitor, leads to mistargeting of tyrosinase to lysosomes and accelerates its degradation. J Invest Dermatol. 129: 1489-1499, 2009.
11) Harsanyi ZP, Post PW, Brinkmann JP, Chedekel MR: Deibel RM.Mutagenicity of melanin from human red hair. Experientia. 36: 291, 1980.
12) Hattori H, Kawashima M, Ichikawa Y, Imokawa G: The epidermal stem cell factor is over-expressed in lentigo senilis: implication for the mechanism of hyperpigmentation. J Invest Dermatol. 122: 1256-1265, 2004.
13) Hida T, Wakamatsu K, Sviderskaya EV, Donkin AJ, Montoliu L, Lynn Lamoreux M, Yu B, Millhauser GL, Ito S, Barsh GS, Jimbow K, Bennett DC: Agouti protein, mahogunin, and attractin in pheomelanogenesis and melanoblast-like alteration of melanocytes: a cAMP-independent pathway. Pigment Cell Melanoma Res. 22: 623-634, 2009.
14) Huizing M, Sarangarajan R, Strovel E, Zhao Y, Gahl WA, Boissy RE: AP-3 mediates tyrosinase but not TRP-1 trafficking in human melanocytes. Mol Biol Cell. 12: 2075-2085, 2001.
15) Ito, S. Fujita, K: Microanalysis of eumelanin and pheomelanin in hair and melanomas by chemical degradation and liquid chromatography. Anal Biochem. 144: 527-536, 1985.
16) Ito S, Fujita K, Takahashi H, Jimbow K: Characterization of melanogenesis in mouse and guinea-pig hair by chemical analysis of melanins and of free and bound dopa and 5-S-cysteinyldopa. J Invest Dermatol. 83: 12-14, 1984.
17) Ito S, Jimbow K: Quantitative analysis of eumelanin and pheomelanin in hair and melanomas. J Invest Dermatol. 80: 268-272, 1983.
18) Jimbow K, Kamiya T, Hida T: Epidermal melanin unit and aging of skin; biological and molecular significance of pheomelanin in constitutive photo-aging process. Geriatric Dermatol Sem. 4: 53-64, 2008.
19) Jimbow K, Chen H, Park JS, Thomas PD: Increased sensitivity of melanocytes to oxidative stress and abnormal expression of tyrosinase-related protein in vitiligo. Br J Dermatol. 144: 55-65, 2001.
20) Jimbow K, Park JS, Kato F, Hirosaki K, Toyofuku K, Hua C, Yamashita T: Assembly, target signal and intracellular transport of tyrosinase gene family proteins in the initial stage of melanosome biogenesis. Pigment Cell Res. 13: 222-229, 2000.

21) Jimbow K, Chen H, Gomez PF, Hirosaki K, Shinoda K, Salopek TG, Matsusaka H, Jin H -Y, Yamashita T: Intracellular vesicular trafficking of tyrosinase gene family protein in eu- and pheomelanosome biogenesis. Pigment Cell Res. 13 (Suppl): 110-117, 2000.
22) Jimbow K: Biolocical role of tyrosinase-related protein and its relevance to pigmentary disorders (vitiligo vulgaris). J Dermatol. 26: 734-737, 1999.
23) Jimbow K, Gomez PF, Toyofuku K, Chang D, Miura S, Tsujiya H, Park JS: Biological role of tyrosinase related protein and its biosynthesis and transport from TGN to stage I melanosome, late endosome, through gene transfection study. Pigment Cell Res. 10: 206-213, 1997.
24) Jimbow K, Salopek TG, Dixon WT, Searles GE, Yamada K: The epidermal melanin unit in the pathophysiology of malignant melanoma. Am J Dermatopath. 13: 179-188, 1991.
25) Jimbow K, Fitzpatrick TB, Quevedo WC Jr: Formation, chemical composition and function of melanin pigments. In: Matoltsy AG, ed. Biology of the integument. Val. II. Springer. 278-292, 1984.
26) Jimbow K, Ishida O, Ito S, Hori Y, Witkop CJ Jr, King RA: Combined chemical and electron microscopic studies of pheomelanosomes in human red hair. J Invest Dermatol. 81: 506, 1983.
27) Jovanovic SV, Simic MG: Redox properties of oxy and audiooxidant radicals. In: Simic MG, Taylor KA, Ward JF, von Sonntag C, eds. Oxygen radicals in biology and medicine. New York: Plenum Press. 115-121, 1988.
28) Kagan VE, Serbinova EA, Packer L: Generation and recycling of radicals from phenolic antioxidants. Arch Biophys. 280: 33-39, 1990.
29) Kalayanaraman B, Felix CC, Sealy RC. Semiquinone anion radicals of catechol (amine) s, catechol estrogens, and their metal complexes. Environ Health Perspect. 64: 185-198, 1985.
30) Koch WH, Chedekel MR: Photoinitiated DNA damage by melanogenic intermediates in vitro. Photochem Photobiol. 44: 703-10, 1986.
31) Lambert C, Land EJ, Riley PA, Truscott TG: A pulse radiolysis investigation of the oxidation of methoxylated metabolities of indolic melanin precursors. Biochim Biophys Acta. 1035: 319-324, 1990.
32) Lambert C, Chacon JN, Chadekel MR, Land EJ, Riley PA, Thompson A, TruscottTG. A pulse radiolysis investigation of the oxidation of indolic melanin precursors: evidence for indolequinones and subsequent intermediates. Biochim Biophys Acta. 933: 12 -20, 1989.
33) Liu TF, Kandala G, Setaluri V: PDZ domain protein GIPC interacts with the cytoplasmic tail of melanosomal membrane protein gp 75 (tyrosinase-related protein-1). J Biol Chem. 276: 35768-35777, 2001.
34) Luo D, Chen H, Jimbow K: Cotransfection of genes encoding human tyrosinase and tyrosinase related protein-1 prevents melanocyte death and enhances melanin pigmentation and gene expression of Lamp-1. Exp Cell Ress. 213: 231-241, 1994.
35) Maresca V, Flori E, Briganti S, Camera E, Cario-Andre M, Taieb A, Picardo M: UVA -induced modification of catalase charge properties in the epidermis is correlated with the skin phototype. J Invest Dermatol. 126: 182-90, 2006.
36) Menon IA, Persad S, Ranadive NS, Haberman HF: Effects of ultraviolet-visible irradiation in the presence of melanin isolated from human black or red hair upon Ehrlich ascites carcinoma cells. Cancer Res. 43: 3165, 1983.
37) Neta P, Steenken S: Phenoxyl radicals: formation, detection, and redox properties in aqueous solutions. In: Rodgers MAJ, Powers EL, eds. Oxygen and oxy-radicals in chemistry and biology. New York: Academic Press. 83-87, 1981.
38) Nordberg J, Arner ES: Reactive oxygen species, antioxidants, and the mammalian thioredoxin system. Free Radic Biol Med. 31: 1287-312, 2001.
39) Orlow SJ, Chakaraborty AK, Pawelek JM: Retinoic acid is a potent inhibitor of inducible pigmentation in murine and hamster melanoma cell lines. J Invest Dermatol. 94: 461-464, 1990.
40) Rad HH, Yamashita T, Jin H-Y, Hirosaki K, Wakamatsu K, Ito S, Jimbow K: Tyrosinase-related proteins suppress tyrosinase-mediated cell death of melanocytes and melanoma cells. Exp Cell Res. 298: 317

-328, 2004.
41) Ranadive NS, Shirwadkar S, Persad S, Menon IA: Effects of melanin-induced free radicals on the isolated rat peritoneal mast cells. J Invest Dermatol. 86: 303-307, 1986.
42) Raposo G, Marks MS: Melanosomes--dark organelles enlighten endosomal membrane transport. Nat Rev Mol Cell Biol. 8: 786-797, 2007
43) Reszka K, Jimbow K: Electron-donor and acceptor properties of melanin pigments in the skin. In: Oxidative Stress In Dermatology, ed by J Fuchs and L Packer, Marcel Dekker Inc, New York. 287-320, 1993.
44) Salopek TG, Yamada K, Ito S, Jimbow K: Dysplastic melanocytic nevi contain high levels of pheomelanin: quantitative comparison of pheomelanin/eumelanin levels between normal skin, common nevi, and dysplastic nevi. Pigment Cell Res. 4: 172-9, 1991.
45) Sato C, Ito S, Takeuchi T: Enhancement of pheomelanogenesis by L-dopa in the mouse melanocyte cell line, TM 10, in vitro. J Cell Sci. 87: 507-512, 1987.
46) Sealy RC, Hyde JS, Felix CC, Menon IA, Prota G: Eumelanins and pheomelanins: characterization by electron spin resonance spectroscopy. Science. 217: 545-547, 1982.
47) Schriner SE, Linford NJ, Martin GM, Treuting P, Ogburn CE, Emond M, Coskun PE, Ladiges W, Wolf N, Van Remmen H, Wallace DC, Rabinovitch PS: Extension of murine life span by overexpression of catalase targeted to mitochondria. Science. 308: 1875-1876, 2005.
48) Simic MG, Desrosiers MF, Hunter EPL: Antioxidant properties of antioxidant dimers. In: Hayaishi O, Niki E, Kondo M, Yoshokawa T, eds. Medical, biochemical and chemical aspects of free radicals. Amsterdam: Elsevier. 433-440, 1989.
49) Steenken S, Neta P: One-electron redox potentials of phenols. Hydroxy-and aminoxyphenols and related compounds of biological interest. J Phys Chem. 86: 3661-3667, 1982.
50) Steenken S, Neta P: Electron transfer rates and equilibria between substituted phenoxide ions and phenoxyl radicals. J Phys Chem. 83: 1134-1137, 1979.
51) Swallow AJ: Physical chemistry of semiquinones. In: Trumpower BL, ed. Function of quinones in energy conserving systems. New York: Academic Press. 59-72, 1982.
52) Takahashi H, Horikoshi T, Jimbow K: Fine structural characterization of melanosomes in dysplastic nevi. Cancer. 56: 111-123, 1985.
53) Theos AC, Tenza D, Martina JA, Hurbain I, Peden AA, Sviderskaya EV, Stewart A, Robinson MS, Bennett DC, Cutler DF, Bonifacino JS, Marks MS, Raposo G: Functions of adaptor protein (AP) -3 and AP-1 in tyrosinase sorting from endosomes to melanosomes. Mol Biol Cell. 16: 5356-5372, 2005.
54) Wood JM, Schallreuter KU: UVA-irradiated pheomelanin alters the structure of catalase and decreases its activity in human skin. J Invest Dermatol. 126: 13-14, 2006.

Biochimica et Biophysica Acta 1800 (2010) 669–673

Contents lists available at ScienceDirect

Biochimica et Biophysica Acta

journal homepage: www.elsevier.com/locate/bbagen

Agaritine purified from *Agaricus blazei* Murrill exerts anti-tumor activity against leukemic cells

Masahiro Endo [a,g,1], Hidehiko Beppu [b,*], Hidehiko Akiyama [c], Kazumasa Wakamatsu [d], Shosuke Ito [d], Yasuko Kawamoto [e], Kan Shimpo [b], Toshimitu Sumiya [f], Takaaki Koike [g], Taei Matsui [a]

[a] *Department of Biology, Faculty of Medical Technology, Fujita Health University School of Health Sciences, Toyoake, Aichi 470-1192, Japan*
[b] *Fujita Memorial Nanakuri Institute, Fujita Health University, Tsu, Mie 514-1296, Japan*
[c] *Department of Clinical Hematology, Faculty of Medical Technology, Fujita Health University of Health Sciences, Toyoake, Aichi 470-1192, Japan*
[d] *Department of Chemistry, Faculty of Medical Technology, Fujita Health University School of Health Sciences, Toyoake, Aichi 470-1192, Japan*
[e] *Department of Microbiology, Faculty of Medical Technology, Fujita Health University School of Health Sciences, Toyoake, Aichi 470-1192, Japan*
[f] *Iwade Research Institute of Mycology, Tsu, Mie 514-0012, Japan*
[g] *Department of Clinical Laboratory Sciences, Faculty of Medical Technology, Fujita Health University School of Health Sciences, Toyoake, Aichi 470-1192, Japan*

ARTICLE INFO

Article history:
Received 13 January 2010
Received in revised form 16 March 2010
Accepted 19 March 2010
Available online 27 March 2010

Keywords:
Agaricus blazei
Agaritine
Anti-tumor activity
Leukemic cell
Non-carcinogenicity

ABSTRACT

Background: Mushrooms of the genus *Agaricus* are a common folk remedy against carcinoma. The active ingredients, polysaccharides and protein-polysaccharide complexes containing β-glucan, have been isolated and shown to have indirect tumor-suppressing activity via an immunological activation.
Methods: The diffusible fraction of a hot-water extract of *Agaricus blazei* Murrill (ABM) powder was fractionated by HPLC based on the anti-tumor activity against leukemic cells *in vitro*. The structure of the anti-tumor substance was determined by NMR and MS analyses.
Results: We purified a tumorcidal substance from the diffusible fraction of ABM and identified it as agaritine, β-*N*-(γ-L(+)-glutamyl)-4-(hydroxymethyl) phenylhydrazine, having a molecular mass of 267 Da. This compound inhibited the proliferation of leukemic cell lines such as U937, MOLT4, HL60 and K562 with IC_{50} values of 2.7, 9.4, 13.0, and 16.0 μg/mL, respectively, but showed no significant effect on normal lymphatic cells at concentrations up to 40 μg/mL. Although agaritine has been suspected of having genotoxic or carcinogenic properties, agaritine did not activate the *umu* gene of *Salmonella*, which reacts to carcinogens.
General significance: The results indicate that agaritine from ABM has direct anti-tumor activity against leukemic tumor cells *in vitro*. This is in contrast to the carcinogenic activity previously ascribed to this compound. Our results also show that this activity is distinct from that of β-glucan, which indirectly suppresses proliferation of tumor cells.

1. Introduction

Mushrooms of the genus *Agaricus* contain, in addition to several minerals, vitamins and dietary fibers, bioactive substances such as immunopotentiating substances which are believed to suppress cancer progression or metastasis [1]. In particular, β-glucan (β1-3, β1-6 linked glucan) from these mushrooms has been reported to act as an immuno-accelerator against cancer cells [2,3]. β-glucans such as lentinan from *Lentinula edodes* [4], schizophyllan from *Schizophyllum commune* [5], and the polysaccharide kureha (krestin) from *Coriolus versicolor* [6] are known to be biological response modifiers for macrophages, T cells and NK cells. These compounds induce the activation of the immune response, and have been clinically used as anti-cancer drugs in combination with other drugs [7–9].

Agaricus blazei Murrill (ABM) is a commonly used folk remedy against carcinoma. The polysaccharides and protein-polysaccharide complexes containing β-glucan have been isolated [1,10,11]. In the present study, we found that the heat-stable and diffusible fraction of ABM has anti-tumor activity *in vitro*. This substance directly decreased the viability of leukemic cell lines but had no effect on normal lymphocytes. Structural analysis revealed that the anti-tumor substance is agaritine, a hydrazine-containing compound. Although a carcinogenic effect of ABM has been reported, and agaritine or metabolic derivatives of agaritine are suspected to be genotoxic,

Abbreviations: ABM, *Agaricus blazei* Murrill; FCS, fetal calf serum; HPLC, high-performance liquid chromatography; MQ water, milli Q water; MS, mass spectrometry; NMR, nuclear magnetic resonance

* Corresponding author. Fujita Memorial Nanakuri Institute, Fujita Health University, 1865 Hisai-isshiki-sho, Tsu, Mie 514-1296, Japan. Tel.: +81 59 252 1010; fax: +81 59 252 0710.
E-mail addresses: hbeppu@fujita-hu.ac.jp (H. Beppu), hakiyama@fujita-hu.ac.jp (H. Akiyama), kwaka@fujita-hu.ac.jp (K. Wakamatsu), sito@fujita-hu.ac.jp (S. Ito), ykawamot@fujita-hu.ac.jp (Y. Kawamoto), shimpo@fujita-hu.ac.jp (K. Shimpo), estrella@iwade101.com (T. Sumiya), tmatsui@fujita-hu.ac.jp (T. Matsui).
[1] Present address: Daiichi-Sankyo RD Associe Co. Ltd., Shinagawa, Tokyo, 140-0001, Japan.

0304-4165/$ – see front matter © 2010 Elsevier B.V. All rights reserved.
doi:10.1016/j.bbagen.2010.03.016

carcinogenic or tumorigenic agents [12–15], the present study shows that, according to the *umu* test, agaritine has no carcinogenic effect. This is the first report that clearly indicates the anti-tumor effects of agaritine *in vitro*.

2. Materials and methods

2.1. Materials

Lyophilized ABM powder was obtained from Nanakuri Institute, Fujita Health University (bulk powder from Iwade Research Institute of Mycology, Tsu, Mie, Japan). Milli Q (MQ) water (Millipore, Tokyo, Japan) was used throughout the experiments. Dialysis membrane, which excludes molecules less than 10 kDa in mass, was purchased from Spectrum Laboratories (Rancho Dominguez, CA, USA). Synthetic agaritine, procarbazine-HCl and other chemicals of the highest purity available were purchased from Wako Pure Chemicals (Osaka, Japan).

2.2. Cells

U937, MOLT4, HL60 and K562 cells were obtained from American Type Culture Collection or Aichi Cancer Research Center (Nagoya, Japan). Cells were cultured in RPMI-1640 medium (Sigma-Aldrich, Tokyo, Japan) supplemented with 10% heat-inactivated fetal calf serum (FCS), 100 units/mL penicillin and 100 μg/mL streptomycin. Cells were placed into 50-cm^2 tissue culture flasks and grown at 37 °C under an atmosphere of 5% CO_2 in air. Peripheral blood mononuclear cells (normal lymphocytes) collected from healthy donors (after receipt of informed consent) were separated by density gradient centrifugation using Isoprep (Robbins Scientific, Sunnyvale, CA, USA) or Histopaque-1077 (Sigma-Aldrich) and cultured in RPMI-1640 medium as above.

2.3. Extraction of the anti-tumor substance

ABM powder (20 g) was boiled in MQ water (2000 mL) for 2 h, and the hot-water extract was chilled, filtrated through Advantech No.2 filter paper (Osaka, Japan) and evaporated to dryness (13.9 g). The dried filtrate was dissolved in MQ water (0.4 g/mL) and dialyzed at 25 °C twice against 750 volumes of MQ water for 2 h, then for 4 h once, using 10 kDa cut off dialysis membrane. The total diffusible fraction was evaporated to dryness and used as the starting material (10.0 g). The remaining solution in the bag (non-diffusible fraction) was also evaporated to dryness (2.1 g).

2.4. Fractionation of the anti-tumor substance by high-performance liquid chromatography (HPLC)

Dry powder of diffusible fraction was dissolved in MQ water (333 mg/mL) and centrifuged at 12,000 rpm for 10 min at 25 °C. The supernatant was passed through a cartridge filter (Millex LCR, 0.2 μm, Millipore) and aliquots (30 mg) were subjected to HPLC on an YMC-Pack ODS AQ column (10 mm × 250 mm, YMC, Kyoto, Japan) equilibrated with MQ water. The column was washed and eluted with a linear gradient of methanol into aqueous MQ water. The eluent was monitored by absorbance (ABS) at 280 nm, and fractions were collected and concentrated by evaporation (after identification of agaritine, a wavelength of 238 nm was used, as this compound shows maximum absorbance at this wavelength). Fractions with anti-tumor activity were subjected to second round of chromatography on an YMC-Pack ODS AQ column (4.7 mm × 250 mm, YMC) equilibrated and eluted with MQ water.

2.5. Structural analysis of the anti-tumor substance

The elucidation of structure of purified substance (3.9 mg) with anti-tumor activity was performed by mass spectrometry (MS), ^{1}H-nuclear magnetic resonance (NMR) and ^{13}C-NMR spectra. Mass analysis was performed by the liquid chromatography/mass spectrometry/mass spectrometry (LC/MS/MS) analysis using an electrospray ionization/ion trap mass spectrometer, an ESI-API 3000 (Applied Biosystems, Carlsbad, CA, USA), and a JMS-700QQ FAB-MS (JEOL, Tokyo, Japan), and NMR was performed at Takara Bio (Ohtsu, Japan) using an Avance 600 (Bruker Biospin, Yokohama, Japan). The MS analysis was carried out directly by the MS/MS at positive ion mode; $[M+H]^+$: m/z 268, 250, 232, 186. ^{1}H-NMR was measured at 600 MHz (D_2O): 2.00 ppm (2H, s), 2.33 ppm (2H, m), 3.60 ppm (1H, s), 4.34 ppm (2H, s), 6.69 ppm (2H, m), 7.09 ppm (2H, m). ^{13}C-NMR was measured at 150 MHz (D_2O): 26.4 ppm (CH_2), 29.8 ppm (CH_2), 54.4 ppm (CH), 63.9 ppm (CH_2OH), 113.7 ppm (CH, aromatic carbon), 129.4 ppm (CH, aromatic carbon), 133.0 ppm (C, aromatic carbon), 147.1 ppm (C, aromatic carbon), 174.2 ppm (COOH), 175.1 ppm (CO). The structure was furthermore clarified by using 2D-NMR and ^{13}C-NMR-DEPT (Distorsionless Enhancement by Polarization Transfer) 135 methods (data not shown).

2.6. Assay for anti-tumor activity

U937, MOLT4, HL60, K562 and normal lymphocyte cells were grown in RPMI-1640 medium containing 10% FCS at 37 °C and 5% CO_2. Cell suspensions (90 μL, 4×10^5/mL) were then incubated with each test solution (10 μL) in a 96-well plate for up to 48 h. Cell survival/proliferation was measured by a Cell Counting Kit-8 (Dojindo, Tokyo, Japan) using water-soluble disulfonated tetrazolium salt (WAT-8) [16]. Briefly, 10 μL of WAT-8 solution was added to each well and the absorbance at 492/620 nm was measured with a Multiskan Bichromatic microplate reader (LabSystems, Bucharest, Romania) after 2 h. Survival rates of the cells were determined and the IC_{50} values were calculated.

2.7. Carcinogenicity test

Carcinogenicity was monitored by the *umu* test using an Umulac AT kit (Jimuro Co. Ltd, Takasaki, Japan) according to the instruction manual [17]. This method is based on the expression of the *umu* gene, which is activated by mutagens. Briefly, a suspension of *Salmonella typhimurium* (NM2009 strain) possessing the *umu* gene conjugated with the β-galactosidase gene was mixed with agaritine (final concentration 1–8 μg/mL) in the presence or absence of cofactor (S9, rat liver homogenate) and incubated for 2 h at 37 °C. Substrate solution (X-gal) was added and absorbance at 620 nm was measured after 1 h. 2-(2-furyl)-3-(5-nitro-2-furyl) acrylamide (2-AF, 0–0.3 μg/mL, without S9) and 2-aminoanthracene (2-AA, 0–0.3 μg/mL, with S9) were used as positive carcinogens.

3. Results

3.1. Purification of the anti-tumor substance

The hot-water extract of ABM suppressed the viability of U937 cells by approximately 40% (Fig. 1). To eliminate high-molecular-weight β-glucan, the hot-water extract was extensively dialyzed against water to separate diffusible small molecules from non-diffusible large molecules. Although the non-diffusible fraction in the dialysis bag showed weak activity at higher concentration, the anti-tumor activity was mainly recovered from the diffusible fraction, indicating that the major anti-tumor substance is a heat-stable small molecule(s) such as a carbohydrate, peptide or other organic compound(s). The diffusible fraction was fractionated by HPLC into five fractions (I–V, Fig. 2A). Since fraction II showed comparatively stronger activity (Fig. 2B), it was repeatedly chromatographed on the HPLC column until a single peak was obtained (Fig. 3A). Finally, 4.1 mg of anti-tumor substance was purified from 20 g of ABM powder. The purified anti-tumor substance showed high tumor-suppression activity, with an IC_{50} value of 6.1 μg/

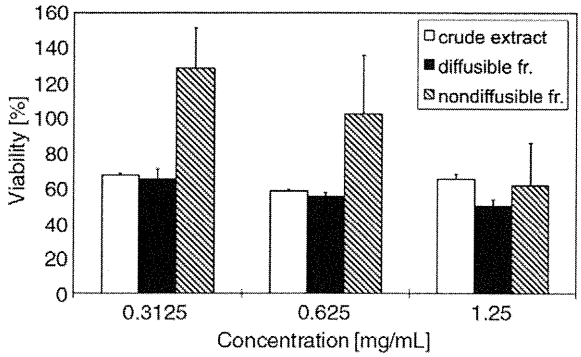

Fig. 1. Effects of ABM extract and dialyzed extract on the viability of U937 cells. Hot-water extract of ABM and diffusible/non-diffusible fractions obtained by extensive dialysis of the hot-water extract were added to U937 cells at concentrations ranging from 0.31 to 1.25 mg/mL. After 48 h, cell viability was assayed using a Cell Counting Kit-8. Anti-tumor activity found in the hot-water extract was largely recovered in the diffusible fraction after dialysis.

mL (Fig. 3B). Since the crude diffusible fraction showed 50% inhibition of U937 proliferation at 1.25 mg/mL (Fig. 1), an approximately 200-fold purification was achieved by the HPLC procedure.

3.2. Structure of the anti-tumor substance

The purified anti-tumor substance was white in color, highly soluble in water, methanol, and ethanol, and showed maximum absorbance at 238 nm. LC/MS analysis showed that it has a molecular mass of 267 Da

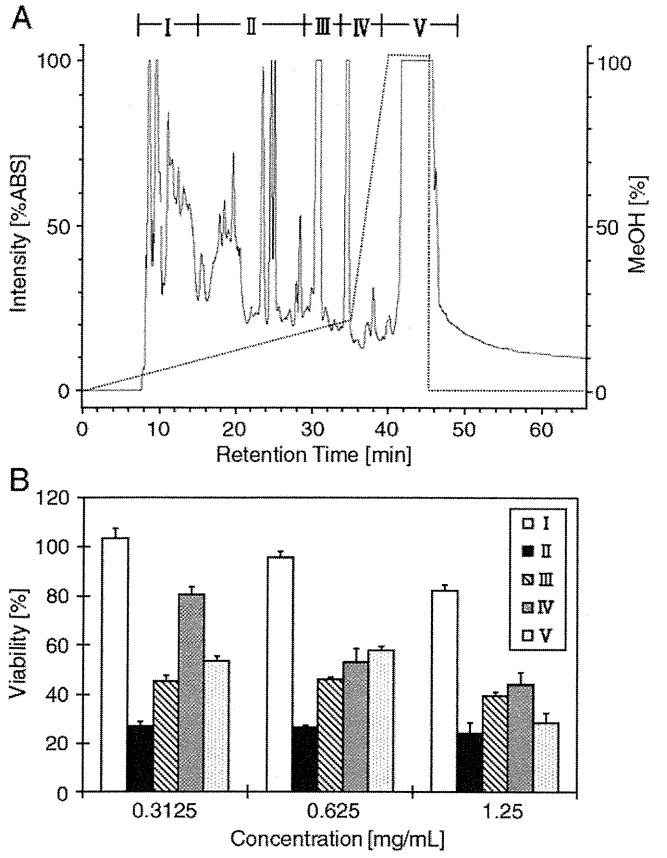

Fig. 2. Fractionation of anti-tumor substances from ABM by HPLC. (A) The diffusible fraction was fractionated into five fractions (I to V) by HPLC on an YMC-Pack ODS AQ column (10 mm×250 mm) using a methanol gradient (dotted line). (B) Each fraction was assayed for cell viability using U-937 cells. Several fractions exhibited anti-tumor activity, with fraction II showing the highest activity.

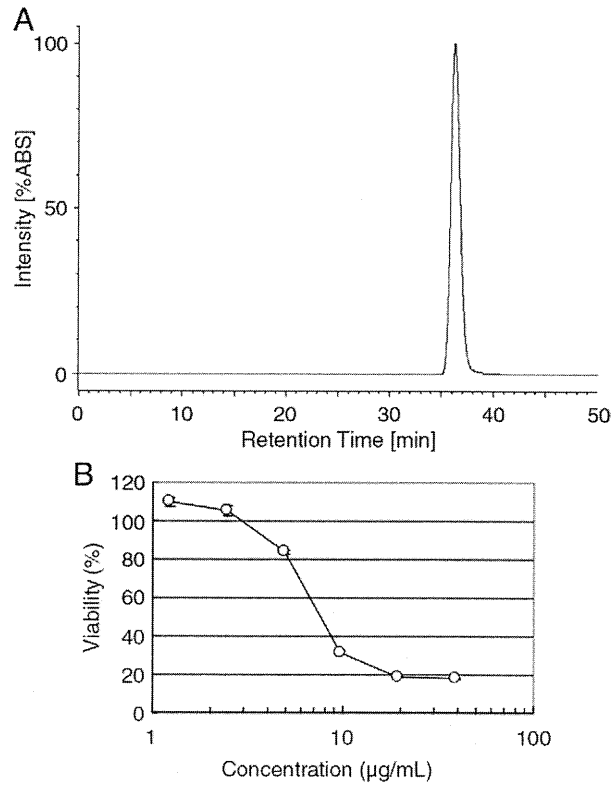

Fig. 3. Purification of the anti-tumor substance. (A): Fraction II in Fig. 2A was repeatedly subjected to HPLC on the same column to provide a single peak fraction. (B) The peak fraction in panel A showed strong suppressive activity towards U937 cells, with an IC_{50} value of 6.1 μg/mL.

(data not shown). ^{13}C-NMR and ^{1}H-NMR analysis, together with the MS data, suggested that the anti-tumor substance is identical to agaritine, β-*N*-(γ-L(+)-glutamyl)-4-(hydroxymethyl) phenylhydrazine ($C_{12}H_{17}O_4N_3$, 267 Da), previously purified from *A. bisporus* [18] and a compound synthesized by Wallcave et al. [19] (Fig. 4). Commercially available synthetic agaritine showed the same retention time and absorbance spectrum as that of the purified anti-tumor substance (data not shown).

3.3. Effects of agaritine on the viability of leukemic cells and normal lymphocytes

Synthetic agaritine was assayed to determine whether it shows anti-tumor activity *in vitro*. As shown in Fig. 5, agaritine suppressed U937 with an IC_{50} value of 2.7 μg/mL, which is comparable to that of the purified anti-tumor substance from ABM. The higher activity of synthetic agaritine suggests that our preparation still contains some

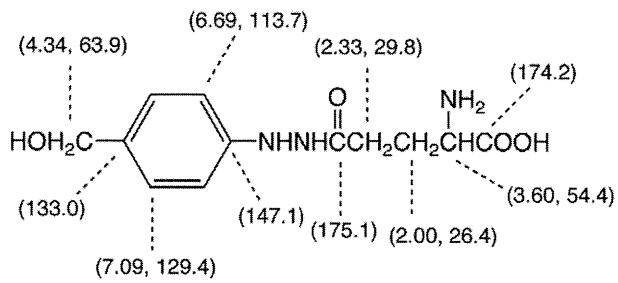

Fig. 4. Structure of the anti-tumor substance isolated from ABM. NMR data of the purified anti-tumor substance were expressed as chemical shift values (ppm) of the ^{1}H-NMR and ^{13}C-NMR (in parentheses) spectra. The anti-tumor substance purified from ABM was identified as phenylhydrazine containing a glutamyl residue. A hydroxymethyl group is located at the *para* position of the benzene ring.

impurities. Since the anti-tumor substance purified from ABM was identified as agaritine, commercial synthetic agaritine was used in the following experiments.

Other leukemic cell lines (K562, MOLT4 and HL60) and normal lymphocytes were incubated with various concentrations of agaritine for 48 h. The viability of all the leukemic cell lines used decreased as the concentration of agaritine increased (Fig. 5). The IC_{50} values of agaritine to MOLT4, HL60 and K562 were 9.4, 13.0, and 16.0 μg/mL, respectively (Fig. 5). Agaritine had no significant effect on the viability of normal lymphocytes at concentrations up to 40 μg/mL (Fig. 5).

3.4. Absence of carcinogenic activity in agaritine

The carcinogenicity of agaritine was examined using the *umu* test (Table 1). Agaritine (1–8 μg/mL) did not activate the *umu* gene of *Salmonella*, which reacts to carcinogens. There was no evidence of carcinogenicity of agaritine even when a cofactor (S9), which metabolically activates promutagens, was added to the *umu* test mixture.

4. Discussion

ABM is a commonly used supplemental health food for suppressing cancer, as well as for preventing hypertension, hyperlipemia and diabetes [1]. Polysaccharides of β1-3, β1-6 linked glucose (β-glucan) found in the genus *Agaricus* have been found to suppress cancer by activating immunological responses of macrophages and leukocytes [2,20]. Recently, direct cytotoxic anti-tumor activity of β-glucan has been reported [21–23]. Since ABM also contains β-glucan [1,10,11], its anti-cancer activity might be due to either a direct or indirect effect by β-glucan. The present study showed that an ABM extract not composed of β-glucan directly suppressed proliferation of leukemic cells *in vitro*. This suppressive activity was concentrated in the heat-stable and dialyzable low molecular weight fractions of ABM. The major anti-tumor substance was identified by structural analysis as agaritine, a phenylhydrazine conjugated with glutamic acid. Commercially available synthetic agaritine also showed the same anti-tumor activity. Several other peaks separated by HPLC showed lower-level anti-tumor activity. There is a possibility that these minor active fractions might contain agaritine derivatives. Indeed, fraction IV (Fig. 2A) contained agaritinal, an agaritine derivative containing an aldehyde side chain instead of a hydroxymethyl group, which also showed anti-tumor activity (data not shown).

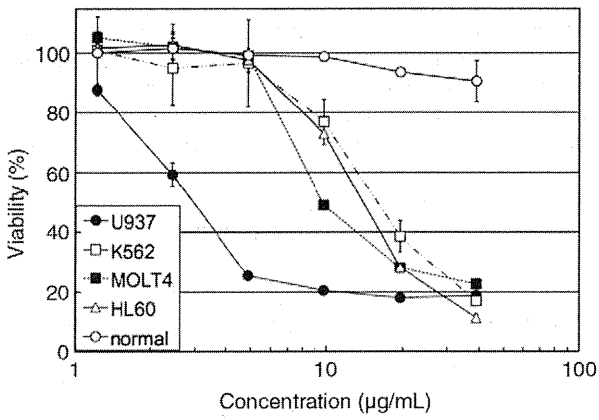

Fig. 5. Anti-tumor activity of agaritine against leukemic cells. Leukemic cells (U937, K562, HL60 and MOLT4) and normal lymphocytes were incubated with 0 to 40 μg/mL of agaritine for 48 h. Cell viability was assessed by using Cell Counting Kit-8. Agaritine showed a suppressive effect on all the leukemic cell lines examined, with IC_{50} values of 2.7, 9.4, 13.0, and 16.0 μg/mL for U937, MOLT4, HL60 and K562, respectively, but showed no significant effect on the normal lymphatic cells at concentrations up to 40 μg/mL. Data represent means of three experiments with SD.

Table 1
Evaluation of carcinogenicity of agaritine by the *umu* test.

Without cofactor S9				With cofactor S9			
AF-2		Agaritine		2-AA		Agaritine	
Conc.	A_{620}	Conc.	A_{620}	Conc.	A_{620}	Conc.	A_{620}
0	0.265	1.0	0.271	0	0.427	1.0	0.452
0.033	0.551	2.0	0.308	0.003	1.034	2.0	0.434
0.1	0.749	4.0	0.255	0.03	2.239	4.0	0.432
0.3	1.498	8.0	0.278	0.3	1.414	8.0	0.398

Carcinogenicity was monitored by the *umu* test using an Umulac AT kit. A suspension of *S. typhimurium* possessing the *umu* gene conjugated with the β-galactosidase gene was mixed with agaritine (final concentration 1–8 μg/mL) in the presence or absence of cofactor S9 and incubated for 2 h at 37 °C. Substrate solution (X-gal) was added and absorbance at 620 nm was measured after 1 h. AF-2 (2-(2-furyl)-3-(5-nitro-2-furyl) acrylamide, 0–0.3 μg/mL) and 2-AA (2-aminoanthracene, 0–0.3 μg/mL) were used as positive control carcinogens for the *umu* test in the absence or presence of cofactor S9, respectively.

Contrary to its anti-tumor effect, agaritine, either purified or from *Agaricus*, has been suspected of promoting carcinogenicity such as bladder cancer [24]. Several reports of Ames test studies using a *Salmonella* strain suggested that agaritine and its derivatives are potentially mutagenic [12]. Administration of agaritine has been reported to induce cancer or tumors in mice [12], but other reports showed that agaritine had no or an insignificant effect [25,26]. The hydrazine structure has also been considered as a carcinogenic reactant. Such conflicting information regarding the carcinogenicity of agaritine has cast doubt on whether commercial supplements from *Agaricus* mushrooms, or the mushrooms themselves, are safe or toxic, leading to the withdrawal of *Agaricus* supplemental products by some companies. Furthermore, it has been reported that agaritine is unstable in boiling water, or easily degrades in water within 48 h [27]. In contrast, in our purification procedure, agaritine was isolated following boiling and exhaustive dialysis in water, indicating that it is stable towards both heat and water, as reported [18]. One explanation for these discrepancies is that the quality and purity of agaritine previously used for experiments were questionable. In 2008, the Japan National Institute of Health Sciences concluded that agaritine has no significant genotoxicity, based on an *in vivo* study using transgenic mice (Food safety commission working group). Our present results using *Salmonella* species (the *umu* test) also show no carcinogenicity of agaritine in the presence or absence of a metabolic modifier, consistent with the results of Papaparaskeva et al. [28]. Although it is not easy to determine the biological effects of agaritine *in vivo*, current evidence suggests that agaritine and its metabolic derivatives are not carcinogenic. Papaparaskeva et al. (1993) suggested that phenolic and quinonoid compounds may play a significant role in the mutagenicity of mushroom extracts [29].

Possible target for agaritine is not clear at present. Since agaritine is an amphipathic molecule, it can presumably easily penetrate the cell membrane. Our chase-experiments using fluorescein-labeled agaritine and U937 cells showed that agaritine was incorporated into the cytoplasm after binding to the cell surface (unpublished results). The anti-tumor activity might be attributable to the hydrazine structure of agaritine, as several hydrazine compounds have been used as anti-cancer drugs. For example, hydrazine sulfate improves cancerous cachexia, and procarbazine (methylhydrazine) has been used to treat leukemia and non-Hodgkin's malignant lymphoma. However, procarbazine has no effect on the viability of U937 *in vitro* (data not shown). Recently, Gao et al. [30] showed by molecular docking experiments that agaritine and its derivatives have a specific potency to bind HIV proteases. Therefore, agaritines are promising candidates for drug-development in the combat of AIDS.

The mechanism by which agaritine decreases the viability of leukemic cells has not been elucidated. In preliminary experiments, we observed nuclear fragmentation and an increase in annexin V-positive U937 cells after incubation with agaritine. These observations

suggest that agaritine induces apoptosis of leukemic cells. Although agaritine showed no toxic effect on normal lymphocytes, we have not examined the effect of agaritine on cancer cell lines other than leukemic cells. Further studies, including cell and species specificity, effective minimum doses for different cells, and *in vivo* administration using an animal model, are necessary to establish the anti-tumor activity and specificity of agaritine.

Acknowledgements

The authors are indebted to Dr. N. Hayashi from Tokyo Institute for Technology for the NMR analysis. This work was supported by a research grant from Fujita Health University.

References

[1] F. Firenzuoli, L. Gori, G. Lombardo, The Medicinal mushroom *Agaricus blazei* Murrill: Review of literature and pharmaco-toxicological problems, Evid-Based Complement. Alternat. Med. 5 (2008) 3–15.
[2] S.P. Wasser, Medicinal mushrooms as a source of antitumor and immunomodulating polysaccharides, Appl. Microbiol. Biotechnol. 60 (2002) 258–274.
[3] D. Akramiene, A. Kondrotas, J. Didziapetriene, E. Kevelaitis, Effects of beta-glucans on the immune system, Medicina (Kaunas) 43 (2007) 597–606.
[4] G. Chihara, J. Hamuro, Y.Y. Maeda, T. Shiio, T. Suga, N. Takasuka, T. Sasaki, Antitumor and metastasis-inhibitory activities of lentinan as an immunomodulator: an overview, Cancer Detect Prev. Suppl. 1 (1987) 423–443.
[5] Y. Sakagami, Y. Mizoguchi, T. Shin, S. Seki, K. Kobayashi, S. Morisawa, S. Yamamoto, Effects of an anti-tumor polysaccharide, schizophyllan, on interferon-gamma and interleukin 2 production by peripheral blood mononuclear cells, Biochem. Biophys. Res. Commun. 155 (1988) 650–655.
[6] M. Harada, K. Matsunaga, Y. Oguchi, H. Iijima, K. Tamada, K. Abe, M. Takenoyama, O. Ito, G. Kimura, K. Nomoto, Oral administration of PSK can improve the impaired anti-tumor CD4+ T-cell response in gut-associated lymphoid tissue (GALT) of specific-pathogen-free mice, Int. J. Cancer 70 (1997) 362–372.
[7] F. Hong, J. Yan, J.T. Baran, D.J. Allendorf, R.D. Hansen, G.R. Ostroff, P.X. Xing, N.K. Cheung, G.D. Ross, Mechanism by which orally administered beta-1, 3-glucans enhance the tumoricidal activity of antitumor monoclonal antibodies in murine tumor models, J. Immunol. 173 (2004) 797–806.
[8] F. Hong, R.D. Hansen, J. Yan, D.J. Allendorf, J.T. Baran, G.R. Ostroff, G.D. Ross, Beta-glucan functions as an adjuvant for monoclonal antibody immunotherapy by recruiting tumoricidal granulocytes as killer cells, Cancer Res. 63 (2003) 9023–9031.
[9] M. Fisher, L.X. Yang, Anticancer effects and mechanisms of polysaccharide-K (PSK): implications of cancer immunotherapy, Anticancer Res. 22 (2002) 1737–1754.
[10] K. Oshiman, Y. Fujimiya, T. Ebina, I. Suzuki, M. Noji, Orally administered beta-1, 6-D-polyglucose extracted from *Agaricus blazei* results in tumor regression in tumor-bearing mice, Planta Med. 68 (2002) 610–614.
[11] Q. Dong, J. Yao, X.T. Yang, J.N. Fang, Structural characterization of a water-soluble beta-D-glucan from fruiting bodies of *Agaricus blazei* Murr, Carbohydr. Res. 337 (2002) 1417–1421.
[12] K. Walton, M.M. Coombs, F.S. Catterall, R. Walker, C. Ioannides, Bioactivation of the mushroom hydrazine, agaritine, to intermediates that bind covalently to proteins and induce mutations in the Ames test, Carcinogenesis 18 (1997) 1603–1608.
[13] B. Toth, D. Nagel, Studies of the tumorigenic potential of 4-substituted phenylhydrazines by the subcutaneous route, J. Toxicol. Environ. Health 8 (1981) 1–9.
[14] O. Sterner, R. Bergman, E. Kesler, G. Magnusson, L. Nilsson, B. Wickberg, E. Zimerson, G. Zetterberg, Mutagens in larger fungi: I. Forty-eight species screened for mutagenic activity in the Salmonella/microsome assay, Mutat. Res. 101 (1982) 269–281.
[15] E.G. Rogan, B.A. Walker, R. Gingell, D.L. Nagel, B. Toth, Microbial mutagenicity of selected hydrazines, Mutat. Res. 102 (1982) 413–424.
[16] M. Ishiyama, Y. Miyazono, K. Sasamoto, Y. Ohkura, K. Ueno, A highly water-soluble disulfonated tetrazolium salt as a chromogenic indicator for NADH as well as cell viability, Talanta 44 (1997) 1299–1305.
[17] Y. Oda, H. Yamazaki, M. Watanabe, T. Nohmi, T. Shimada, Development of high sensitive umu test system: rapid detection of genotoxicity of promutagenic aromatic amines by *Salmonella typhimurium* strain NM2009 possessing high *O*-acetyltransferase activity, Mutat. Res. 334 (1995) 145–156.
[18] B. Levenberg, Isolation and structure of agaritine, a gamma-glutamyl-substituted arylhydrazine derivative from Agaricaceae, J. Biol. Chem. 239 (1964) 2267–2273.
[19] L. Wallcave, D.L. Nagel, C.R. Raha, H.-S. Jae, S. Bronczyk, R. Kupper, B. Toth, An improved synthesis of agaritine, J. Org. Chem. 44 (1979) 3752–3755.
[20] A.T. Borchers, J.S. Stern, R.M. Hackman, C.L. Keen, M.E. Gershwin, Mushrooms, tumors, and immunity, Proc. Soc. Exp. Biol. Med. 221 (1999) 281–293.
[21] Y. Fujimiya, Y. Suzuki, K. Oshiman, H. Kobori, K. Moriguchi, H. Nakashima, Y. Matumoto, S. Takahara, T. Ebina, R. Katakura, Selective tumoricidal effect of soluble proteoglucan extracted from the basidiomycete, *Agaricus blazei* Murill, mediated via natural killer cell activation and apoptosis, Cancer Immunol. Immunother. 46 (1998) 147–159.
[22] E. Jimenez-Medina, E. Berruguilla, I. Romero, I. Algarra, A. Collado, F. Garrido, A. Garcia-Lora, The immunomodulator PSK induces in vitro cytotoxic activity in tumour cell lines via arrest of cell cycle and induction of apoptosis, BMC Cancer 8 (2008) 78.
[23] Y. Gu, Y. Fujimiya, Y. Itokawa, M. Oshima, J.S. Choi, T. Miura, T. Ishida, Tumoricidal effects of beta-glucans: mechanisms include both antioxidant activity plus enhanced systemic and topical immunity, Nutr. Cancer 60 (2008) 685–691.
[24] C. Hashida, K. Hayashi, L. Jie, S. Haga, M. Sakurai, H. Shimizu, Quantities of agaritine in mushrooms (*Agaricus bisporus*) and the carcinogenicity of mushroom methanol extracts on the mouse bladder epithelium, Nippon Koshu Eisei Zasshi 37 (1990) 400–405.
[25] K. Pilegaard, E. Kristiansen, O.A. Meyer, J. Gry, Failure of the cultivated mushroom (*Agaricus bisporus*) to induce tumors in the A/J mouse lung tumor model, Cancer Lett. 120 (1997) 79–85.
[26] S.E. Shephard, C. Schlatter, Covalent binding of agaritine to DNA in vivo, Food Chem. Toxicol. 36 (1998) 971–974.
[27] J. Hajslova, L. Hajkova, V. Schulzova, H. Frandsen, J. Gry, H.C. Andersson, Stability of agaritine—a natural toxicant of Agaricus mushrooms, Food Addit. Contam. 19 (2002) 1028–1033.
[28] C. Papaparaskeva, C. Ioannides, R. Walker, Agaritine does not mediate the mutagenicity of the edible mushroom *Agaricus bisporus*, Mutagenesis 6 (1991) 213–217.
[29] C. Papaparaskeva-Petrides, C. Ioannides, R. Walker, Contribution of phenolic and quinonoid structures in the mutagenicity of the edible mushroom *Agaricus bisporus*, Food Chem. Toxicol. 31 (1993) 561–567.
[30] W.N. Gao, D.Q. Wei, Y. Li, H. Gao, W.R. Xu, A.X. Li, K.C. Chou, Agaritine and its derivatives are potential inhibitors against HIV proteases, Med. Chem. 3 (2007) 221–226.

Cancer Science
The official journal of the Japanese Cancer Association

Melanoma-targeted chemo-thermo-immuno (CTI)-therapy using *N*-propionyl-4-*S*-cysteaminylphenol-magnetite nanoparticles elicits CTL response via heat shock protein-peptide complex release

Akiko Sato,[1] Yasuaki Tamura,[2,6] Noriyuki Sato,[2] Toshiharu Yamashita,[1] Tomoaki Takada,[1] Makito Sato,[1] Yasue Osai,[1] Masae Okura,[1] Ichiro Ono,[1] Akira Ito,[3] Hiroyuki Honda,[4] Kazumasa Wakamatsu,[5] Shosuke Ito[5] and Kowichi Jimbow[1]

Departments of [1]Dermatology and [2]Pathology, Sapporo Medical University, Sapporo; [3]Department of Chemical Engineering, Faculty of Engineering, Kyusyu University, Fukuoka; [4]Department of Biotechnology, Nagoya University, Nagoya; [5]Department of Chemistry, Fujita Health University, Toyoake, Japan

(Received February 1, 2010/Revised April 22, 2010/Accepted May 4, 2010/Accepted manuscript online May 19, 2010/Article first published online June 28, 2010)

Melanogenesis substrate, *N*-propionyl-4-*S*-cysteaminylphenol (NPrCAP) is specifically taken up by melanoma cells and inhibits their growth by producing cytotxic free radicals. By taking advantage of this unique chemical agent, we have established melanoma-targeting intracellular hyperthermia by conjugating NPrCAP with magnetite nanoparticles (NPrCAP/M) upon exposure to an alternating magnetic field (AMF). This treatment causes cytotoxic reaction as well as heat shock responses, leading to elicitation of antitumor immune response, which was proved by tumor rechallenge test and CTL induction. We found the level of heat shock protein 72 (Hsp72) to be increased in the cell lysate and culture supernatant after intracellular hyperthermia. Melanoma-specific CD8$^+$ T-cell response to dendritic cells loaded with hyperthermia-treated tumor lysate was enhanced when compared with non-treated tumor lysate. When heat shock protein, particularly Hsp72, was immuno-depleted from hyperthermia-treated tumor cell lysate, specific CD8$^+$ T-cell response was abolished. Thus, it is suggested that antitumor immune response induced by hyperthermia using NPrCAP/M is derived from the release of HSP-peptide complex from degraded tumor cells. Therefore, this chemo-thermo-immuno (CTI)-therapy might be effective not only for primary melanoma but also for distant metastasis because of induction of systemic antimelanoma immune responses. (*Cancer Sci* 2010; 101: 1939–1946)

Melanoma has been increasing in incidence leading to a rise in morbidity and mortality in recent decades. Metastatic melanoma is extremely difficult to cure and continues to have a poor prognosis. Only 12% with metastatic melanoma survive for 5 years.[1] The reason for this poor prognosis is the lack of effective conventional therapies. Various types of therapies such as immunotherapy, chemotherapy, and biologic therapy have been studied in melanoma management. However, a very modest effect was recorded in advanced malignant melanoma. Therefore, there is an emerging need for innovative therapies for the control of advanced melanoma.

It has been reported that the intracellular hyperthermia using magnetic nanoparticles is effective for treating certain types of cancer in not only primary but also metastatic lesions.[2–8] Incorporated magnetic nanoparticles generate heat within the cells after exposure to the alternating magnetic field (AMF) due to hysteresis loss or relaxational loss.[9,10] One of us has shown that hyperthermic treatment using magnetite cationic liposomes (MCLs), which are cationic liposomes containing 10-nm magnetite nanoparticles, induces antitumor immunity by enhancement of heat shock protein (HSP) expression.[3,11–13] We previously proposed that cross-presentation of extracellular HSP-peptide complex released from hyperthermia-induced necrotic tumor cells is the mechanism for inducing antitumor immunity.[7] In this paper, we present evidence that tumor-derived HSP-peptide complex is responsible for the hyperthermia-mediated antitumor immunity.

In addition, exploitation of biological properties unique to melanoma cells may provide a novel approach to improve the effect of hyperthermic treatment. We have previously shown that the sulfur-amine analog of tyrosine, 4-S-cysteaminyl phenol (4-*S*-CAP), and its *N*-acetyl or propionyl derivatives (NAcCAP or NPrCAP) are good substrates for melanoma-specific targeting and therapy. They have been shown to cause selective cytotoxicity against melanocytes and melanoma cells after selective uptake. Therefore, they can be good candidates for developing antimelanoma chemotherapy because melanogenesis is inherently toxic and expressed uniquely in melanocytic cells.[14–17] Recently, we synthesized new magnetite nanoparticles, NPrCAP/M, on which NPrCAP was directly conjugated on the surface of magnetite nanoparticles.[18,19] We have shown that NPrCAP/M is specifically targeted to melanoma cells, and internalized and aggregated within their cell cytoplasm. In addition, we have observed that B16 melanoma cells, which were subjected to intracellular hyperthermia using NPrCAP/M with AMF exposure, were brought to necrotic cell death, resulting in tumor growth retardation.[18] Here we show that the intracellular hyperthermic treatment using NPrCAP/M with AMF exposure induces tumor-specific immune responses and therefore we call this antimelanoma therapy "chemo-thermo-immuno (CTI)" therapy. We demonstrate that CTI therapy-induced antimelanoma immunity is mediated through cross-presentation of up-regulated intracellular and extracellular HSPs-peptide complex derived from melanoma cells.

Materials and Methods

Mice and cells. Female C57BL/6 mice were obtained from Hokudo (Sapporo, Japan) and used at 4–6 weeks of age.

[6]To whom correspondence should be addressed.
E-mail: ytamura@sapmed.ac.jp

doi: 10.1111/j.1349-7006.2010.01623.x

B16-OVA is a B16F1 melanoma cells stably transfected with chicken ovalbumin (OVA) cDNA (kindly provided by Dr Y. Nishimura, Kumamoto University, Kumamoto, Japan). B16-OVA was cultured in DMEM supplemented 10% FCS and 250 μg/mL of hygromycin B. B3Z is a $CD8^+$ T-cell hybridoma that expresses LacZ in response to activation of T-cell receptors specific for the SIINFEKL peptide (SL8; OVA-immunodominant peptide) in the context of $H\text{-}2K^b$ (kindly provided by Dr N. Shastri, University of California, Berkeley, CA, USA). B16F1 melanoma cells, CT26 colon carcinoma cells, and LLC lung carcinoma cells were cultured in DMEM supplemented with 10% FCS. EL4 lymphoma cells, YAC-1 cells, and B3Z cells were cultured in complete RPMI supplemented with 10% FCS. Bone marrow-derived dendritic cells (DCs) were generated from the femurs and tibiae of C57BL/6 mice. The bone marrow was flushed out, and the leukocytes were obtained and cultured in complete RPMI-1640 with 10% FCS and 20 ng/mL GM-CSF (Endogen, Woburn, MA, USA) for 5 days. On day 3, fresh medium with GM-CSF was added to the plates for the day 5 cultures.

Preparation of NPrCAP/M. Magnetite nanoparticles (Fe_3O_4; average particle size, 10 nm) were kindly provided by Toda Kogyo (Hiroshima, Japan). The details of the preparation of NPrCAP/M are described elsewhere.[18] Briefly, magnetite nanoparticles were coated with aminosilane and conjugated with NPrCAP via maleimide cross-linkers. The resultant NPrCAP/M was suspended in 10 mL of H_2O. The degree of incorporation of NPrCAP to magnetite was 61.0 nmol/mg magnetite.

Antibodies. For depletion of HSPs from cell lysate, anti-Hsp72/Hsc73 mAb, anti-Hsp90α polyclonal antibody, anti-Hsp90 mAb, and anti-lysine-aspartic acid-glutamic acid-leucine (KDEL) mAb were used. Anti-Hsp72/Hsc73 mAb and anti-Hsp90mAb were used for western blotting. These antibodies were obtained from StressGen Biotechnologies Victoria, BC, Canada). Mouse IgG and Rabbit IgG were purchased from IBL (Takasaki, Japan).

Measurement of iron concentration in the NPrCAP/M-exposed cells. Subconfluently growing melanoma and non-melanoma cells ($8 \times 10^4/cm^2$) in a 25-cm^2 flask were re-fed with the medium containing 5.94 mg of NPrCAP/M or magnetite (84 mg/mL). To discriminate between incorporation of NPrCAP/M and magnetite by direct attachment to cells and that by diffusion from the medium, culture flasks were fixed on a slanted disc and rotated slowly for 30 min. After the cells were washed with PBS twice and collected, they were dissolved completely in 200 μL of concentrated HCl and incubated at 43°C for 30 min. Then, 10 mL of H_2O_2 and 4 mL of 1% potassium thiocyanate were added in sequence to the cell solution. The concentration of NPrCAP/M used in these experiments was 24.4 μM as NPrCAP.

Transplantation of tumor cells and intracellular hyperthermia. All of the animal experiments were conducted with the approval of the Animal Experiment Ethics Committee of Sapporo Medical University. B16-OVA cells (1×10^6) were subcutaneously transplanted into the right flank of C57BL/6 mice on day 0. NPrCAP/M nanoparticles (24.4 μM as NPrCAP, 100 μL) were injected subcutaneously into the tumor on days 7, 9, 11, and 13. A magnetic field was created using a horizontal coil (inner diameter, 7 cm; length, 7 cm) with a transistor inverter (LTG-100-05; Dai-ichi High Frequency, Tokyo, Japan).[4] The magnetic field frequency and intensity were 118 KHz and 30.6 KA/m (386 Oe), respectively. Twenty-four hours after injection, mice were subjected to AMF exposure to heat the tumor at 43°C for 30 min. The heated field was three dimensions, which was created using a horizontal coil with a transistor inverter. The mice whose tumors were injected with NPrCAP/M were put in a horizontal coil and exposed to AMF. Moreover, we monitored the temperature of the tumor surface as well as the rectal temperature using an optical fiber probe. The temperature of the tumor surface was maintained at 43°C and rectal temperature was about 38°C. Tumor growth was recorded once every 2 days. The cured mice were then rechallenged with a subcutaneous injection of B16-OVA cells (1×10^6) or irrelevant 3LL lung carcinoma cells (1×10^6) on the left flank. Tumor size was determined by the following formula: tumor volume = $0.5 \times (\text{length} \times \text{width}^2)$, where length and width were measured in millimeters.

Histopathology of tumor sections. Twenty-one days after tumor challenge, subcutaneous B16-OVA tumors were harvested and fixed in 10% formalin in PBS, then paraffin embedded and sectioned. Hematoxylin–eosin (H&E)-stained sections were prepared for analysis of therapeutic effect and gross infiltrate. For immunohistochemical analysis, the frozen tissues were stained with an antimouse CD4 mAb (Santa Cruz Biotechnology, Santa Cruz, CA, USA) or an antimouse CD8 mAb (Chemicon International, Temecula, CA, USA) and then incubated with HRP-conjugated goat antirat Ig (Dako, Tokyo, Japan), followed by hematoxylin counterstaining.

***In vitro* cytotoxicity assay.** After mice were treated by intracellular hyperthermia as described above, spleens were harvested on day 28, then 5×10^6 spleen cells were restimulated *in vitro* with irradiated B16-OVA cells in 2 mL of RPMI-1640 supplemented with 50 μM of β-mercaptethanol (Invitrogen, Carlsbad, CA, USA) and 10% FCS for 5 days. Cytotoxic activity of the effector cells against target cells (B16-OVA, EL4, EL4 loaded with SL8 peptide and YAC-1) was determined by standard ^{51}Cr release assay.

Quantification of HSPs. Cultured B16-OVA cells were exposed to NPrCAP/M for 30 min and irradiated by AMF to heat them at 43°C. After NPrCAP/M exposure with or without AMF irradiation, cells (1×10^6) were cultured in 1 mL of 10% RPMI for 72 h. Culture supernatant was collected at 12, 24, and 48 h, or cells escaping cell death were lysed at 72 h after intracellular hyperthermia by freezing and thawing and centrifugation at 2380 *g* for 5 min. The expression of Hsp72/Hsc73 and Hsp90 was determined by western blotting with an anti-Hsp72/Hsc73 mAb or anti-Hsp90 mAb. Heat shock protein (HSP) in the lysate or culture supernatant was quantified by the Hsp90α ELISA and Hsp70 ELISA kits (StressGen), which can detect and quantify Hsp90α and inducible Hsp72, respectively.

Cross-presentation of antigen derived from hyperthermia-treated tumor cell lysate by DCs. Cultured B16-OVA cells were exposed to NPrCAP/M for 30 min and irradiated by AMF to heat them at 43°C. After NPrCAP/M exposure with or without AMF irradiation, cells were cultured for 72 h and 1×10^7 of cells in 1 mL of 10% RPMI medium were lysed by three cycles of freezing and thawing and centrifugation at 2380*g* for 5 min. Dendritic cells DCs (1×10^5) derived from bone marrow of C57BL/6 mice were pulsed with the cell lysate (100 μL) and incubated with 1×10^5 B3Z T cell hybridoma. After overnight incubation, LacZ activity was measured by addition of 100 μL of chlorophenol red-β-D-galactopyranoside (CPRG, Roche, Basel, Switzerland) solution. The absorbance was measured at 595 nm after 4-h incubation at 37°C.

Immunodepletion of HSP. Cultured B16-OVA cells were treated and lysed as described above. The cell lysate (100 μL) was incubated with antibodies (5 μg each) against Hsp90, Hsp72/Hsc73, KDEL, or all of them. The mixture was added to 10 μL of protein A-Sepharose beads (50% slurry; GE Healthcare Japan, Tokyo, Japan), and the suspension was rotated at RT for 1 h. Then, the suspension was spun at 14 000*g* for 1 min. After removal of the beads, the supernatant was used for cross-presentation assay using B3Z as described above. Mouse IgG (15 μg) was used as an experimental control. Depletion was assessed by immunoblotting with anti-Hsp90, Hsp72/Hsc73, or KDEL antibodies.

doi: 10.1111/j.1349-7006.2010.01623.x

***In vivo* cross-presentation of antigen derived from melanoma cells after CTI therapy.** B16-OVA cells (1×10^6) were transplanted into the footpads of C57BL/6 mice on day 0. NPrCAP/M nanoparticles (24.4 μM as NPrCAP, 100 μL) were injected into the tumor on days 7, 9, 11, and 13. Twenty-four hours after injection, mice were subjected to AMF exposure to heat the tumor at 43°C for 30 min. Control mice were injected with PBS or NPrCAP/M nanoparticles alone without hyperthermia. After 5 h of the last CTI therapy against B16-OVA, popliteal nodes were removed and DCs were isolated using CD11c MACS beads (Miltenyi Biotec).Then, B3Z cells (1×10^5) were added to the DC culture (1×10^5) in 96-well flat-bottom plates and incubated at 37°C. Twenty-four hours after incubation, absorbance at 595 nm was measured.

Statistical analyses. All experiments were independently performed three times in triplicate. Comparisons between two groups were performed using Student's *t*-test. In the tumor transplantation assay, we determined statistical significance using Kruskal–Wallis one-way analysis. In all experiments, differences were considered statistically significant at $P < 0.05$.

Results

***N*-propionyl-4-*S*-cysteaminylphenol with magnetite nanoparticles (NPrCAP/M) was preferentially incorporated into melanoma cells.** To examine whether NPrCAP/M could be incorporated into melanoma cells more preferentially than magnetite alone, we compared amounts of iron molecules in cells after culture in the NPrCAP/M- or magnetite-containing media. As shown in Figure 1, B16F1, B16-OVA melanoma cells incorporated large amounts of iron derived from NPrCAP/M compared to that from magnetite alone. Non-melanoma CT26 colon carcinoma and LLC lung carcinoma cells captured a small amount of NPrCAP/M; however, the amount was not significantly different from that with magnetite alone or was almost the same as for magnetite. These data suggested that NPrCAP/M nanoparticle was an ideal agent for specific targeting to melanoma cells.

Antitumor effect of intracellular hyperthermia using NPrCAP/M with AMF exposure and its ability to induce antitumor immunity. We have recently reported the efficacy of melanoma growth inhibition by combination therapy of NPrCAP/M administration with AMF exposure.[19] B16F1 melanoma bearing mice treated with NPrCAP/M injection followed by hyperthermia showed apparent tumor growth retardation. In addition, we have observed that treatment with NPrCAP/M alone (without hyperthermia) also showed the growth suppression of B16F1 melanoma, indicating that NPrCAP/M has a chemotherapeutic effect. In this paper, we used B16-OVA, which was B16 melanoma transfected with OVA as a surrogate tumor antigen, to examine the antigen-specific antitumor immune response. Mice were transplanted with B16-OVA melanoma cells and treated with NPrCAP/M injection followed by hyperthermia or NPrCAP/M injection alone as described in the Materials and Methods. Histopathological examination of the day 21 tumors without treatment showed that inflammatory infiltrates were poorly detected including $CD8^+$ T cells and $CD4^+$ T cells (Fig. 2a-i, -ii, -iii, -iv). In contrast, treatment with combination of NPrCAP/M injection and hyperthermia induced apparent tumor destruction and necrosis with deposit of NPrCAP/M particles (Fig. 2a-v, -vi). In addition, a dense inflammatory infiltrate including neutrophiles, macrophages, plasma cells, and lymphocytes was observed around the residual tumor cells (Fig. 2a-vii, -viii). Furthermore, we have observed that this infiltrate included both $CD8^+$ T cells and $CD4^+$ T cells (Fig. 2a-ix, -x). These T cells were hardly seen around the tumor without treatment or with NPrCAP/M without AMF exposure (data not shown). Tumor volume in the group treated by combination of NPrCAP/M injection and hyperthermia was significantly reduced compared with the non-treated control group ($P = 0.0025$) and the group of NPrCAP alone ($P = 0.023$) (Fig. 2b). Six out of 10 mice in the group treated by NPrCAP/M injection and hyperthermia were cured. In contrast, all mice died of tumor burden in the treatment with NPrCAP/M without AMF and control groups. Interestingly, both NPrCAP/M with and without AMF exposure resulted in a significant and equal reduction of melanoma tumor volume by 17 days after tumor challenge. However, the tumors of mice treated with NPrCAP/M without AMF exposure grew rapidly after day 17. This suggested that hyperthermia might be required for the complete elimination of melanoma tumors. To examine whether cured mice developed antitumor immune responses, these mice were rechallenged with live B16-OVA melanoma cells or irrelevant mouse lung carcinoma LLC 4 weeks after NPrCAP/M and hyperthermic treatment. As a result, all cured mice rejected a rechallenge of live B16-OVA melanoma cells, but not LLC lung carcinoma cells (Fig. 2c). These data indicated that intracellular hyperthermia using NPrCAP/M with AMF exposure induced specific antitumor immunity.

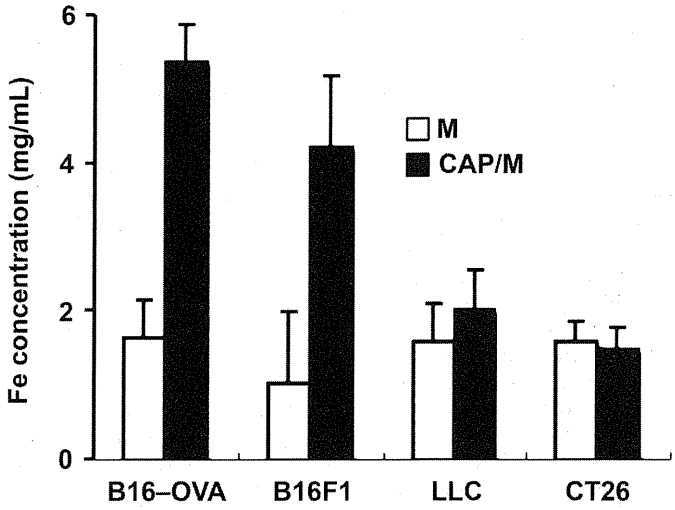

Fig. 1. *N*-propionyl-4-*S*-cysteaminylphenol with magnetite nanoparticles (NPrCAP/M) was preferentially incorporated into melanoma cells. Subconfluently growing melanoma and non-melanoma cells ($8 \times 104/cm^2$) in a 25 cm^2 flask were fed with medium containing 5.94 mg of NPrCAP/M or magnetite (84 mg/mL) for 30 min. Iron concentration of magnetite nanoparticles was measured using the potassium thiocyanate method.

Induction of tumor-specific CTL by intracellular hyperthermia. To analyze the mechanism for the generation of antitumor immunity by NPrCAP/M and hyperthermia, we examined CTL induction in mice after intracellular hyperthermia. Spleen cells of mice after hyperthermia showed high cytotoxicity against B16-OVA melanoma cells compared to EL4 lymphoma and YAC-1 cells. In addition, spleen cells also showed high cytotoxicity against EL4 pulsed with SL8 peptide derived from OVA protein (Fig. 3). These results suggest that intracellular hyperthermia using NPrCAP/M can elicit specific tumor immunity by inducing CTL against B16-OVA melanoma cells.

Enhanced expression of Hsp72 in B16-OVA melanoma cell after intracellular hyperthermia. We examined the expression of HSPs in tumor cells treated with NPrCAP with AMF exposure *in vitro* by western blotting and ELISA. The protein level of Hsp72 but not Hsc73 or Hsp90 was increased at 48 h after hyperthermia (Fig. 4a). Similarly, the concentration of Hsp72 in cell lysate resulted in a three-fold increase at 72 h after hyperthermia, compared to cells without treatment (Fig. 4b). However, the concentration of Hsp90 did not change (Fig. 4c).

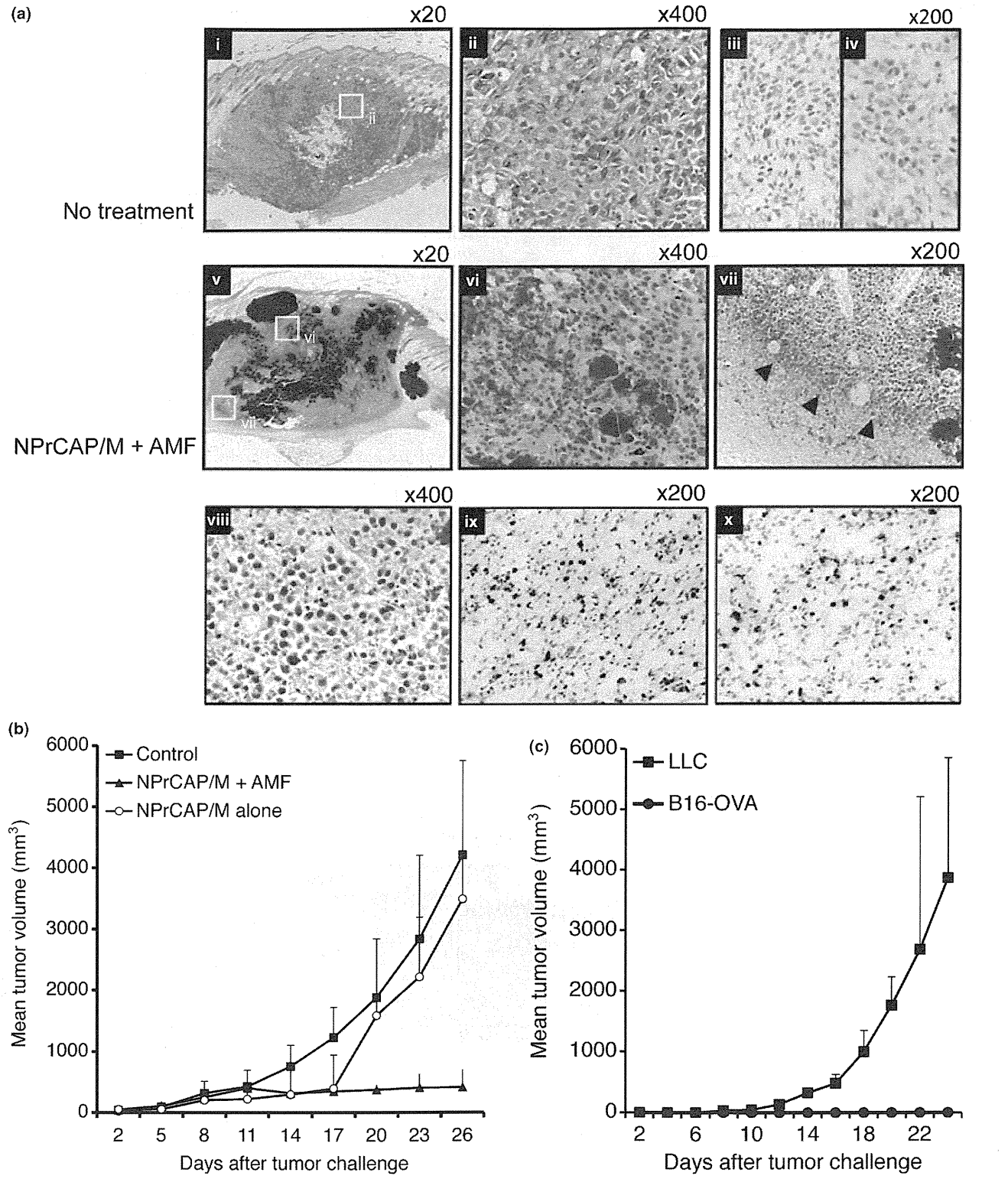

Fig. 2. Antitumor effect and tumor-specific immunity induced by intracellular hyperthermia using *N*-propionyl-4-*S*-cysteaminylphenol with magnetite nanoparticles (NPrCAP/M) and alternating magnetic field (AMF) exposure. (a) Pre-established subcutaneous B16-OVA tumors without treatment (i,ii,iii,iv) or intracellular hyperthermia using NPrCAP/M with AMF exposure (v,vi,vii,viii,ix,x) were harvested and analyzed histologically using H&E-stained sections. Intracellular hyperthermia using NPrCAP with AMF exposure induced tumor destruction and inflammatory infiltrate (arrow head). The frozen tissues excised from mice untreated or treated with NPrCAP/M with AMF exposure were stained with an antimouse CD8 mAb (iii,ix) or CD4 mAb (iv,x). (b) Tumor growth of B16-OVA melanoma cells in non-treated control mice (n = 10), mice treated with NPrCAP/M with AMF exposure (n = 10), or mice treated with NPrCAP/M alone (n = 10). Points, mean tumor volume (mm^3); bars, SD. (c) The development of tumor specific immunity by intracellular hyperthermia. Mice cured by intracellular hyperthermia were rechallenged with B16-OVA melanoma cells (n = 3) or lung carcinoma LLC (n = 3). Mice were transplanted with 1×10^6 B16-OVA cells and then the tumor growth rates of each group were compared using the average tumor size. Points, mean tumor volume (mm^3); bars, SD. Results shown are representative of three different experiments.

doi: 10.1111/j.1349-7006.2010.01623.x

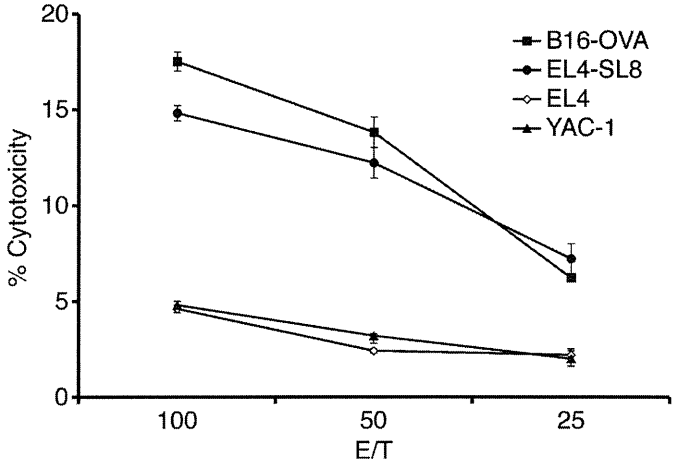

Fig. 3. Induction of tumor-specific CTL by intracellular hyperthermia. Analysis of spelenocytes cytotoxic activity against B16-OVA melanoma cells, EL4, EL4 pulsed with SL8 peptide, and YAC-1 in ^{51}Cr release assay. Mice were treated by *N*-propionyl-4-*S*-cysteaminylphenol with magnetite nanoparticles (NPrCAP/M) injection followed by alternating magnetic field (AMF) exposure. Four weeks after treatment, spleen cells were removed and stimulated with irradiated B16-OVA cells. Cytotoxic activity of spleen cells against B16-OVA cells, EL4 cells, EL4 cells pulsed with SL8 peptide, or YAC-1 cells was determined by standard ^{51}Cr-release assay. Bars, SD.

Treatment with NPrCAP alone decreased the level of intracellular Hsp72 and Hsp90. We are currently investigating the underlying mechanism. From the results obtained, we hypothesized that hyperthermia using NPrCAP/M might induce tumor immunity through up-regulation of Hsp72.

Intracellular hyperthermia using NPrCAP/M with AMF exposure results in the release of HSPs into the extracellular milieu. It has been demonstrated that once cancer cells become necrotic, several HSPs, above all, Hsp72 and Hsp90, are released from cells and might act as a danger signal, subsequently eliciting cell-specific immune responses. We therefore examined whether Hsp72 and Hsp90 would be released from necrotic melanoma cells after intracellular hyperthermia *in vitro*. Culture supernatants from B16-OVA were collected at 12, 24, and 48 h after intracellular hyperthermia and the quantity of Hsp72 and Hsp90 was evaluated using ELISA. Although Hsp72 and Hsp90 were detected at 48 h after hyperthermia, concentration of extracellular Hsp72 was a 4.5-fold higher than that of Hsp90 (Fig. 4d). These *in vitro* results suggested that treatment of B16-OVA melanoma with intracellular hyperthermia would release HSPs, in particular Hsp72, into extracellular milieu *in vivo* and these extracellular HSPs might play an important role in inducing antitumor immunity.

$CD8^+$ T-cell response against DCs loaded with B16-OVA melanoma cell lysate after intracellular hyperthermia. To analyze the mechanism of tumor specific CTL induction, we examined B3Z $CD8^+$ T-cell response against DCs loaded with supernatant from B16-OVA culture after intracellular hyperthermia. However, only a very modest response was observed (data not shown). One of the reasons for this modest response may be the degradation of peptide chaperoned by HSPs by protease in the culture medium. We therefore decided to use melanoma cell lysate after hyperthermia. NPrCAP/M loaded B16-OVA melanoma cells were subjected to AMF irradiation and cultured for 72 h. Melanoma cells were lysed by three cycles of freezing and thawing. Dendritic cells (DCs) derived from mouse bone marrow were loaded with the lysate for 2 h and then cultured with B3Z $CD8^+$ T-cell hybridoma. B3Z response against DC loaded with B16-OVA melanoma cell lysate increased after intracellular hyperthermia using NPrCAP/M, compared with non-heated cells and cells loaded NPrCAP/M without AMF exposure (Fig. 5a). These data demonstrated that loading DCs with lysate derived from melanoma cells treated with hyperthermia enhanced the cross-presentation of B16-OVA-specific antigen peptide.

Effects of immunodepletion of HSPs on $CD8^+$ T-cell response. Next, we investigated the underlying mechanism

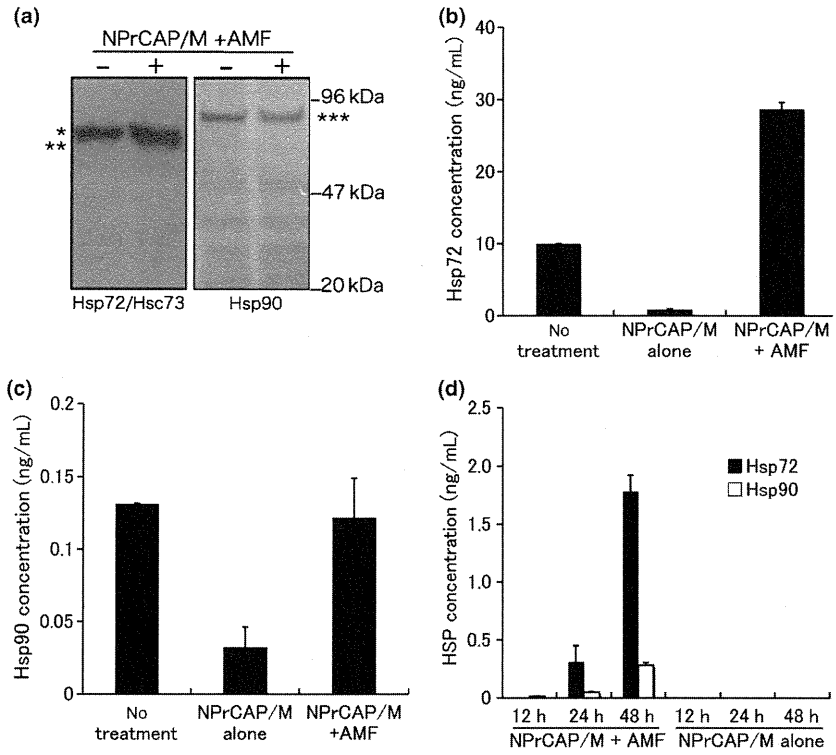

Fig. 4. Heat shock protein (HSP) expression in tumor cells after intracellular hyperthermia. (a–c) B16-OVA cells were subjected to hyperthermia using *N*-propionyl-4-*S*-cysteaminylphenol with magnetite nanoparticles (NPrCAP/M) with alternating magnetic field (AMF) exposure *in vitro*. Seventy-two hours after intracellular hyperthermia (+) or left untreated (–), the expression of Hsp72 and Hsp90 was determined by western blotting with an anti-Hsp72/Hsc73 mAb or anti-Hsp90 mAb (a). *Hsc73, **Hsp72, ***Hsp90. The expression of Hsp72 was markedly enhanced by intracellular hyperthermia. Heat shock protein (HSP) in the lysate was quantified by the Hsp72 ELISA (b) and Hsp90 ELISA kits (c). (d) Hsp72 and Hsp90 in the 12-, 24- and 48-h culture supernatant after intracellular hyperthermia were measured using ELISA. Bars, SD. Results shown are representative of three different experiments.

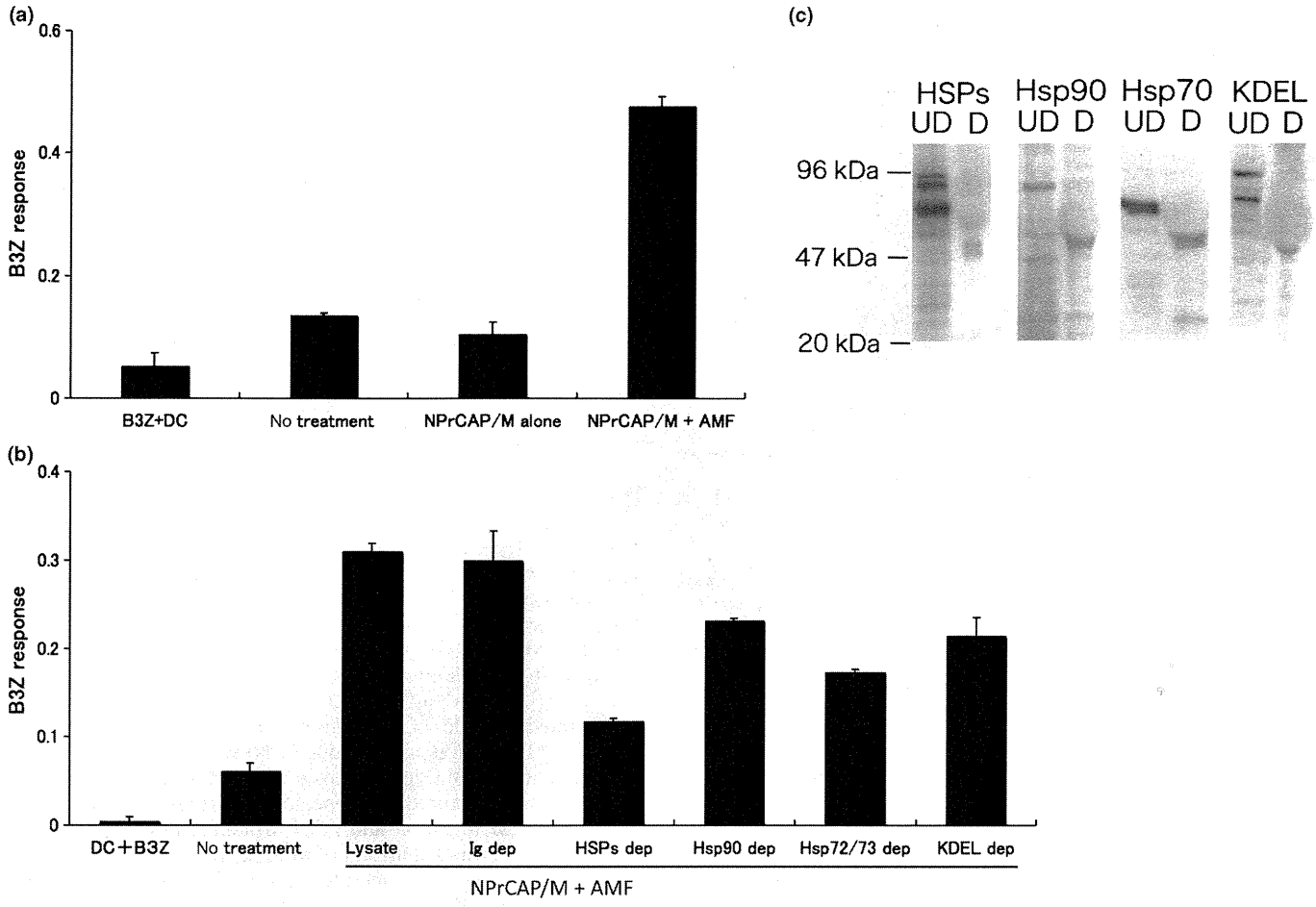

Fig. 5. $CD8^+$ T-cell response against dendritic cells (DCs) pulsed with B16-OVA melanoma cell lysate after intracellular hyperthermia and effect of heat shock protein (HSP) depletion. (a) B16-OVA cells were subjected to *N*-propionyl-4-*S*-cysteaminylphenol with magnetite nanoparticles (NPrCAP/M) exposure and alternating magnetic field (AMF) irradiation, then lysed by freezing and thawing. Dendritic cells (DCs) were pulsed with the cell lysate, and cultured overnight with B3Z and the absorbance of β-galactosidase activity was measured at 595 nm. Bars, SD. (b) Lysates of the cells were immunoprecipitated with anti-Hsp72/Hsc73 antibody, anti-Hsp90 antibody and anti-KDEL antibody. Immunoprecipitates were removed from lysate. After being pulsed with the HSP-depleted lysate, DCs were incubated with B3Z T cell hybridoma and the absorbance of β -galactosidase activity was measured at 595 nm. Bars, SD. (c) Cell lysates were depleted of HSPs (above lanes) with antibodies specific for each HSP. Immunoblots were of depleted (D) or undepleted (UD) lysates. Results shown are representative of five different experiments.

responsible for the enhancement of cross-presentation by intracellular hyperthermia. Hyperthermia has long been shown to induce the expression of HSPs within tumor cells, which have been shown to chaperone tumor-associated antigen peptides. To investigate the role of HSPs in intracellular hyperthermia-induced $CD8^+$ T-cell response, we depleted HSPs from lysate using anti-HSP antibody, and measured $CD8^+$ T-cell response against DCs loaded with the HSP-depleted lysate. Depletion of major HSPs (Hsp72/Hsc73, Hsp90, and ER-resident HSPs) from NPrCAP/M and hyperthermic treated B16-OVA cell lysate caused a loss of 59% of initial B3Z response ($P = 0.0001$ *vs* depletion with control Ig) (Fig. 5b), whereas depletion with control Ig did not show any effect. Importantly, depletion of Hsp72/Hsc73 exhibited a 44% reduction of activity and it was best decreased in response in the HSP depletion assay. The inhibition rate was statistically significant compared with the depletion with control Ig ($P = 0.001$). Depletion of Hsp90 or ER resident HSPs caused a loss of 25% ($P = 0.0857$) or 31% ($P = 0.0034$) of the initial activity, respectively. Immunoblots showed that depletion of each HSP was complete (Fig. 5c). These results suggested that Hsp72/Hsc73, Hsp90, and ER-resident HSPs were involved in the induction of CTL response at various extents. In addition, our data demonstrated that these HSPs chaperoned antigenic peptides and extracellular HSP-peptide complexes were cross-presented by DCs, followed by specific CTL activation. Notably, Hsp72/Hsc73 was largely responsible for the observed T-cell response. As shown in Figure 4, these data were consistent with the enhanced expression of Hsp72 within the melanoma cells. Thus, DCs loaded with intracellular hyperthermia-treated melanoma cell lysate are more efficient than DCs loaded with untreated melanoma cell lysate in cross-presentation to CTLs.

Dendritic cells (DCs) derived from tumor-draining lymph nodes cross-present melanoma-associated antigen after CTI therapy. We examined whether melanoma-associated antigen was indeed cross-presented by DCs within tumor-draining lymph nodes after CTI therapy. To test this, we transplanted B16 melanoma cells into the footpads of mice. After three rounds of CTI therapy, tumor-draining popliteal nodes were removed and DCs were isolated and cultured with B3Z. B3Z response against regional lymph node-derived DCs of CTI-treated mice was evident when compared to PBS control or NPrCAP/M injection without hyperthermia (Fig. 6). We therefore conclude that intracellular hyperthermia using NPrCAP/M with

doi: 10.1111/j.1349-7006.2010.01623.x

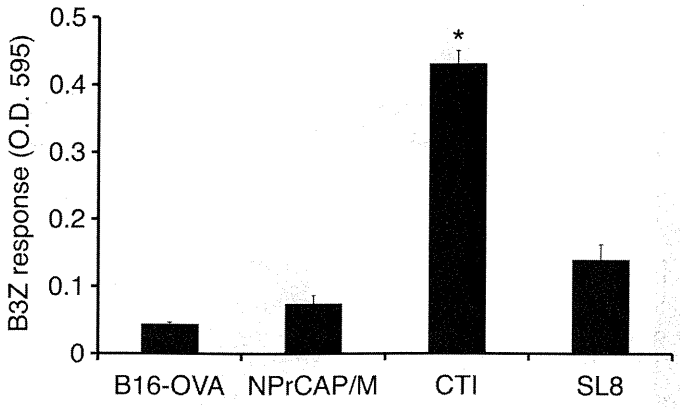

Fig. 6. Dendritic cells (DCs) derived from tumor-draining lymph nodes cross-present melanoma-associated antigen after CTI therapy. B16-OVA cells (1×10^6) were transplanted into the footpads of C57BL/6 mice on day 0. *N*-propionyl-4-*S*-cysteaminylphenol with magnetite nanoparticles (NPrCAP/M) nanoparticles (24.4 mM as NPrCAP, 100 mL) were injected into the tumor on days 7, 9, 11, and 13. Twenty-four hours after injection, mice were subjected to alternating magnetic field (AMF) exposure to heat the tumor at 43°C for 30 min. Control mice were injected with PBS or NPrCAP/M nanoparticles alone without hyperthermia. After 5 h of the last CTI therapy against B16-OVA, tumor-draining popliteal nodes were removed and DCs were isolated, then cultured with B3Z cells. Twenty-four hours after incubation, absorbance at 595 nm was measured. Bars, SD. $*P < 0.01$; paired Student's *t*-test. Data are representative of three independent experiments.

AMF exposure promotes OVA-derived peptide presentation on DCs both *in vitro* and *in vivo*.

Discussion

In this study, we showed that intracellular hyperthermia of melanoma cells using NPrCAP/M with AMF exposure elicited antitumor immune responses via cross-presentation of HSP-chaperoned antigen. Moreover, we demonstrated that DCs derived from tumor-draining lymph nodes indeed cross-presented melanoma-associated antigen after CTI therapy. It has been believed that enhanced expression of intracellular HSPs by hyperthermia plays an important role in the induction of antitumor immunity.[11,20] Moreover, it has been demonstrated that overexpression of HSPs, particularly Hsp72, causes increased tumor immunogenicity due to augmentation of the chaperoning ability of antigenic peptide, thereby augmenting the presentation of antigenic peptide in the context of MHC class I molecules.[21,22] However, in order to prime tumor-specific immunity, it is necessary to present tumor antigen in the context of MHC class I in conjunction with the co-stimulation signal through co-stimulatory molecules such as B7.1 and B7.2 by professional antigen-presenting cells such as DCs. Dendritic cells (DCs) have the unique capacity to take up, process, and present exogenous antigens in association with MHC class I molecules. This process is termed cross-presentation and the resulting $CD8^+$ T-cell priming is referred to as cross-priming. It has been demonstrated that some exogenous antigens such as HSPs[23–27] and particulate protein antigens[28] gain access to the MHC class I processing pathway and initiate CTL responses. This exogenous pathway is important for the development of $CD8^+$ CTL responses against tumors and infectious pathogens that do not have access to the classical MHC class I pathway.

Here, we showed that the HSPs-antigen peptide complex released from melanoma cells treated with intracellular hyperthermia is taken up by DCs and cross-presented HSP-chaperoned peptide in the context of MHC class I molecules (Fig. 7). Our CTI therapy induced NPrCAP- as well as heat-mediated melanoma cell necrosis to NPrCAP/M incorporated cells. We have reported that repeated hyperthermia (three cycles of NPrCAP/M injection and AMF irradiation) was required to induce the maximal antitumor immune responses.[19] If melanoma cells escape from necrotic cell death, repeated hyperthermia should produce necrotic cell death of previously heat shocked-melanoma cells in which HSPs were induced. In fact, our data suggested that Hsp72/Hsc73, Hsp90, and ER-resident

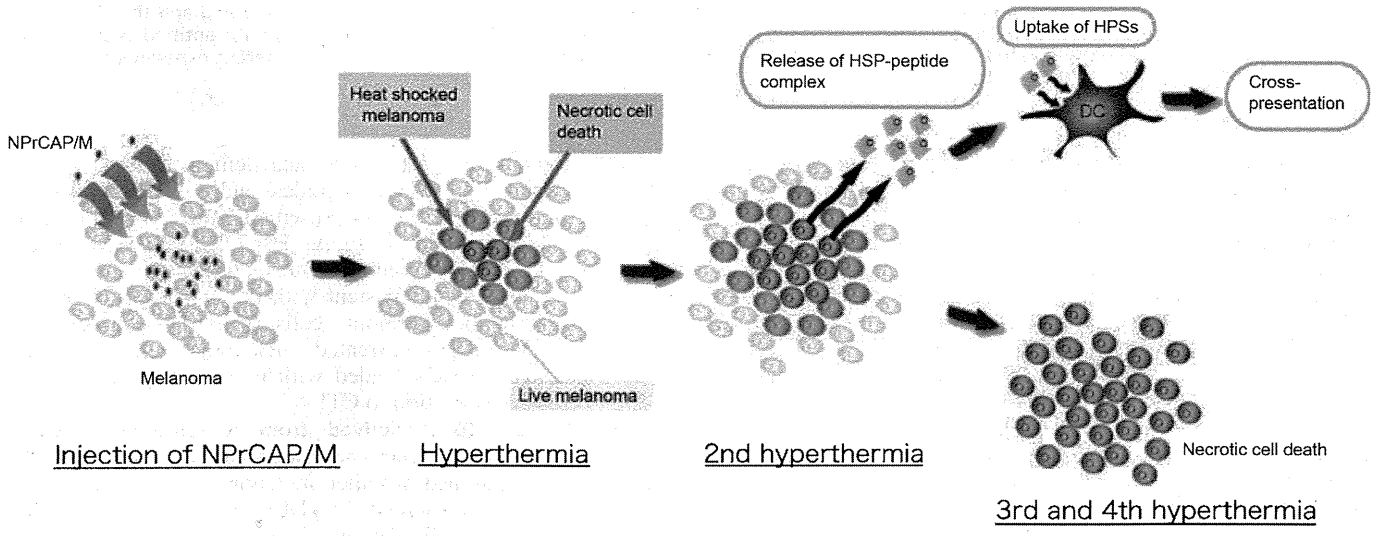

Fig. 7. Schema of intracellular hyperthermia using *N*-propionyl-4-*S*-cysteaminylphenol with magnetite nanoparticles (NPrCAP/M) with alternating magnetic field (AMF) exposure. Injected NPrCAP/M nanoparticles are specifically incorporated in melanoma cells. Intracellular hyperthermia can induce necrotic cell death and adjacent live melanoma cells suffer heat shock, resulting in increased level of intracellular heat shock protein (HSP)-peptide complexes. Repeated hyperthermia turns heat-shocked cells to necrotic cells, leading to the release of their intracellular contents, including HSPs-peptide complexes, into extracellular milieu. The released HSPs-peptide complexes are taken up by dendritic cells (DCs). Then, DCs migrate into regional lymph nodes and cross-present HSP-chaperoned antigenic peptides to $CD8^+$ T cells in the context of MHC class I molecules, thereby inducing antimelanoma CTLs. Finally, the remaining melanoma cells are killed by repeated hyperthermia or by the melanoma-specific CTLs.

HSPs participated in the induction of $CD8^+$ T-cell response. In particular, among HSPs, Hsp72 was largely responsible for the augmented antigen presentation to $CD8^+$ T cells. As Hsp72 is known to up-regulate in response to hyperthermia or heat shock treatment,[11] newly synthesized Hsp72 has a chance to bind to the heat-denatured melanoma-associated antigen.

Taken together, intracellular hyperthermia using NPrCAP/M is a promising treatment for improvement of clinical effects, especially for patients with advanced metastatic melanomas, and even for prevention of recurrence and/or metastasis for early melanomas because of induction of systemic antimelanoma immunity.

Acknowledgments

We thank Dr Shastri for providing B3Z T cell hybridoma, Dr Nishimura for providing B16-OVA, and Toda Kogyo Co. for providing the magnetite. This work was supported by a Health and Labor Sciences Research Grant-in-Aid for Research on Advanced Medical Technology from the Ministry of Health, Labor and Welfare of Japan.

Disclosure Statement

The authors have no conflict of interest.

References

1 Balch CM, Buzaid AC, Soong SJ *et al.* Final version of the American Joint Committee on Cancer staging system for cutaneous melanoma. *J Clin Oncol* 2001; **19**: 3635–48.
2 Yanase M, Shinkai M, Honda H, Wakabayashi T, Yoshida J, Kobayashi T. Intracellular hyperthermia for cancer using magnetite cationic liposomes: an in vivo study. *Jpn J Cancer Res* 1998; **89**: 463–9.
3 Kawai N, Ito A, Nakahara Y *et al.* Anticancer effect of hyperthermia on prostate cancer mediated by magnetite cationic liposomes and immune-response induction in transplanted syngeneic rats. *Prostate* 2005; **64**: 373–81.
4 Ito A, Shinkai M, Honda H, Kobayashi T. Medical application of functionalized magnetic nanoparticles. *J Biosci Bioeng* 2005; **100**: 1–11.
5 Yanase M, Shinkai M, Honda H, Wakabayashi T, Yoshida J, Kobayashi T. Antitumor immunity induction by intracellular hyperthermia using magnetite cationic liposomes. *Jpn J Cancer Res* 1998; **89**: 775–82.
6 Ito A, Shinkai M, Honda H, Wakabayashi T, Yoshida J, Kobayashi T. Augmentation of MHC class I antigen presentation via heat shock protein expression by hyperthermia. *Cancer Immunol Immunother* 2001; **50**: 515–22.
7 Ito A, Kobayashi T, Honda H. A mechanism of antitumor immunity induced by hyperthermia. *Jpn J Hyperthermic Oncol* 2005; **21**: 1–19.
8 Ito A, Takeshi K. Intracellular hyperthermia using magnetite nanoparticles: a novel method for hyperthermia clinical applications. *Thermal Medicine* 2008; **24**: 113–29.
9 Shinkai M, Yanase M, Honda H, Wakabayashi T, Yoshida J, Kobayashi T. Intracellular hyperthermia for cancer using magnetite cationic liposomes: in vitro study. *Jpn J Cancer Res* 1996; **87**: 1179–83.
10 Hergt R, Dutz S, Mueller R, Zeisberger M. Magnetite particle hyperthermia: nanoparticle magnetism and materials development for cancer therapy. *J Phys Condens Matter* 2006; **18**: S2919–34.
11 Ito A, Shinkai M, Honda H *et al.* Heat shock protein 70 expression induces antitumor immunity during intracellular hyperthermia using magnetite nanoparticles. *Cancer Immunol Immunother* 2003; **52**: 80–8.
12 Ito A, Matsuoka F, Honda H, Kobayashi T. Antitumor effects of combined therapy of recombinant heat shock protein 70 and hyperthermia using magnetic nanoparticles in an experimental subcutaneous murine melanoma. *Cancer Immunol Immunother* 2004; **53**: 26–32.
13 Ito A, Honda H, Kobayashi T. Cancer immunotherapy based on intracellular hyperthermia using magnetite nanoparticles: a novel concept of "heat-controlled necrosis" with heat shock protein expression. *Cancer Immunol Immunother* 2006; **55**: 320–8.
14 Ito Y, Jimbow K. Selective cytotoxicity of 4-S-cysteaminylphenol on follicular melanocytes of the black mouse: rational basis for its application to melanoma chemotherapy. *Cancer Res* 1987; **47**: 3278–84.
15 Miura S, Ueda T, Jimbow K, Ito S, Fujita K. Synthesis of cysteinylphenol, cysteaminylphenol, and related compounds, and in vivo evaluation of antimelanoma effect. *Arch Dermatol Res* 1987; **279**: 219–25.
16 Miura T, Jimbow K, Ito S. The in vivo antimelanoma effect of 4-S-cysteaminylphenol and its n-acetyl derivative. *Int J Cancer* 1990; **46**: 931–4.
17 Thomas PD, Kishi H, Cao H *et al.* Selective incorporation and specific cytocidal effect as the cellular basis for the antimelanoma action of sulphur containing tyrosine analogs. *J Invest Dermatol* 1999; **113**: 928–34.
18 Sato M, Yamashita T, Ohkura M *et al.* N-propionyl- cysteaminylphenol - magnetite conjugate (NPrCAP/M) is a nanoparticle for the targeted growth suppression of melanoma cells. *J Invest Dermatol* 2009; **129**: 2233–41.
19 Takada T, Yamashita T, Sato M *et al.* Growth inhibition of re-challenge B16 melanoma transplant by conjugates of melanogenesis substrate and magnetite nanoparticles as the basis for developing melanoma-targeted chemo-thermo-immunotherapy. *J Biomed Biotechnol* 2009; **2009**: 457936.
20 Mise K, Kan N, Okino T *et al.* Effect of heat treatment on tumor cells and antitumor effector cells. *Cancer Res* 1990; **50**: 6199–202.
21 Wells AD, Rai SK, Salvato MS, Band H, Malkovsky M. Hsp72-mediated augmentation of MHC class I surface expression and endogenous antigen presentation. *Int Immunol* 1998; **10**: 609–17.
22 Ito A, Matsuoka F, Honda H, Kobayashi T. Heat shock protein 70 gene therapy combined with hyperthermia using magnetic nanoparticles. *Cancer Gene Ther* 2003; **10**: 918–25.
23 Udono H, Srivastava PK. Comparison of tumor-specific immunogenicities of stress-induced proteins gp96, hsp90, and hsp70. *J Immunol* 1994; **152**: 5398–403.
24 Tamura Y, Peng P, Liu K, Daou M, Srivastava PK. Immunotherapy of tumors with autologous tumor-derived heat shock protein preparations. *Science* 1997; **278**: 117–20.
25 Moroi Y, Mayhew M, Treka J *et al.* Induction of cellular immunity by immunization with novel hybrid peptides complexed to heat shock protein 70. *Proc Natl Acad Sci USA* 2000; **97**: 3485–90.
26 Kurotaki T, Tamura Y, Ueda G *et al.* Efficient Cross-Presentation by Heat Shock Protein 90-Peptide Complex-Loaded Dendritic Cells via an Endosomal Pathway. *J Immunol* 2007; **179**: 1803–13.
27 Kutomi G, Tamura Y, Okuya K *et al.* Targeting to static endosome is required for efficient cross-presentation of endoplasmic reticulum-resident oxygen-regulated protein 150-peptide complexes. *J Immunol* 2009; **183**: 5861–9.
28 Shen L, Sigal LJ, Boes M, Rock KL. Important role of cathepsin S in generating peptides for TAP-independent MHC class I crosspresentation in vivo. *Immunity* 2004; **21**: 155–65.

doi: 10.1111/j.1349-7006.2010.01623.x